Green Chemistry

ROYAL SOCIETY OF CHEMISTRY

CRITICAL REVIEW

View Article Online
View Journal | View Issue

Cite this: *Green Chem.*, 2024, **26**, 11406

Catalytic hydrodeoxygenation and C–C coupling of lignin and its derivatives into renewable jet-fuel-range cycloalkanes

Xinyong Diao, [a,b] Ying Xiong,[a] Yawen Shi,[a] Longlong Ma, [c] Chenglong Dong,[d] Shengbo Zhang [a] and Na Ji *[a]

Cycloalkanes with the carbon numbers C9–C16 are ideal jet-fuel components and are mainly synthesized by the hydrogenation of petroleum-derived benzenes and the cyclization reactions of linear alkanes. The catalytic conversion of lignin and its derivatives, intrinsically embodying carbocyclic structures, to jet-fuel-range cycloalkanes has been demonstrated as a potential green and economical route, which can improve the sustainability of sustainable aviation fuels (SAFs) as well as reduce the overall greenhouse gas emissions. Direct hydrodeoxygenation (HDO) as well as C–C coupling relay hydrodeoxygenation are the two main routes for the production of cycloalkanes from lignin and its derivatives. In this review, first, the HDO of lignin C–O derivatives to monocycloalkanes over metal–acid catalysts was considered a model reaction to provide an understanding of the catalytic structure–activity relationship of the indispensable HDO process. Then, the production of lignin jet fuel *via* the simultaneous depolymerization and HDO of real lignin was discussed, followed by the C–C coupling relay hydrodeoxygenation route for polycycloalkanes production, including the alkylation relay hydrodeoxygenation route, aldol condensation relay hydrodeoxygenation route and one-pot conversion route. Furthermore, this paper attempts to highlight the remaining challenges and provide some perspectives for the future design of structure-specific cycloalkanes, aiming to provide insights into the viable utilization of lignin to obtain C9–C16 ideal jet-fuel-range cycloalkanes.

Received 25th April 2024,
Accepted 15th October 2024

DOI: 10.1039/d4gc02051k

rsc.li/greenchem

1 Introduction

The decline in fossil fuel resources and growing concerns about the environmental problems caused by uncontrolled carbon dioxide emissions from human activities have prompted the search for sustainable and environmentally friendly alternative energy sources. Solar, wind, hydro, and biomass energy are gaining more and more attention as renewable energy sources. Some of these energy sources are intermittent and require large-scale infrastructure. In contrast, biomass-based liquid fuels do not require extensive changes to existing facilities due to their similarity to the currently preferred fuel sources.[1]

Cycloalkanes are an essential component of fossil fuels, accounting for 30–40 wt% of diesel,[2,3] 20 wt% of jet fuel (Fig. 1a),[4] and 10 wt% of gasoline.[5] Generally, cycloalkanes with different total carbon numbers, C6 ring numbers and side-chain substitutions present significant difference in fuel density, flash points, boiling point, freezing point, *etc*. Therefore, the structural requirement of cycloalkanes for diesel, jet fuel, and gasoline are quite different. In the past decades, cycloalkanes have been mainly synthesized by the hydrogenation of petroleum-derived benzenes and the cyclization reactions of linear alkanes (Fig. 1b). Thus, it is crucial to develop more green and sustainable synthetic routes. Recently, the catalytic conversion of lignin and its derivatives, intrinsically embodying carbocyclic structures, has been demonstrated as a potential green and economical route for the production of cycloalkanes.

Considering the space and working environment of aviation aircraft, jet fuel is usually required to meet high standards, including high fuel density (>0.8 g mL^{-1}), low freezing point, flash point >38 °C, and boiling point <300 °C. These standards define the structure and composition of jet-fuel-range cycloalkanes. The typical cycloalkane compounds of the conventional

[a]*School of Environmental Science and Engineering, Tianjin Key Laboratory of Biomass/Wastes Utilization, Tianjin University, Tianjin 300350, China. E-mail: jina@tju.edu.cn*
[b]*The Key Laboratory of Functional Molecular Solids, Ministry of Education, Anhui Normal University, Wuhu 241000, China*
[c]*Key Laboratory of Energy Thermal Conversion and Control of Ministry of Education, School of Energy and Environment, Southeast University, Nanjing 210096, PR China*
[d]*Sinopec Research Institute of Petroleum Processing, Beijing 100083, China*

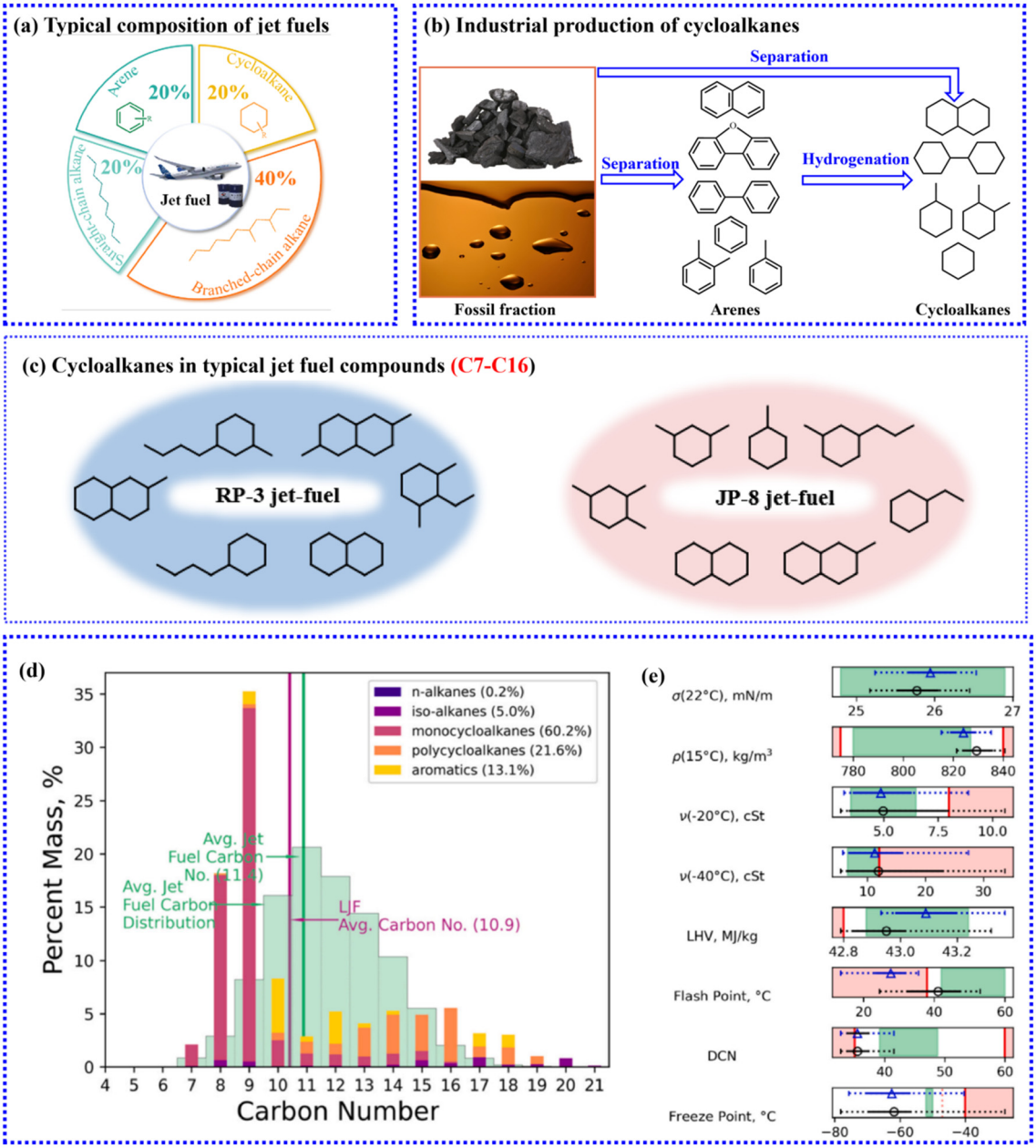

Fig. 1 (a) Composition of jet fuel;[4] (b) industrial production of cycloalkanes; (c) cycloalkanes in typical jet fuel components;[9–11] (d) hydrocarbon-type analysis of lignin-based jet fuel (LJF) and the average conventional jet fuel carbon distribution (green shaded region); (e) tier α predictions on full distillate LJF (blue triangle and lines) and virtual distilled LJF (black circle and lines), with the conventional fuel experience range (green shaded region), ASTM D7566 specification limit (red bar), and violation of the specification (red shaded region) shown for reference. Reproduced from ref. 7 with permission. Copyright 2024, Elsevier.

RP-3 and JP-8 jet fuels are shown in Fig. 1c, involving C7–C10 alkylated monocyclohexanes and C10–C12 polycycloalkanes. Table 1 shows the carbon number of the typical cycloalkane fraction in Jet A-1, demonstrating a carbon distribution of cycloalkanes as C7–C13.[6] It also has been reported that the average conventional jet fuel carbon distribution is C7–C17 (Fig. 1d), and the average carbon number is 11.4.[7] However, it should be noted that an elevated concentration of light hydrocarbons (≤C8) would result in the violation of the flash point (Fig. 1e).[7] In detail, the flash points of methylcyclohexane (C7) and ethylcyclohexane (C8) are −3 °C and 18.9 °C, respectively, which are well below the standard requirement of 38 °C. The flash point of propylcyclohexane is 35 °C, which is near the range and thus can be present in jet fuel to some extent. Therefore, C9+ monocyclohexanes are considered as good components of jet fuel. Also, C7–C8 cycloalkanes if present in small portions only will not greatly affect the fuel properties of the jet fuel. Other standards also limit the structural of polycy-

Table 1 Mass content [wt%] of hydrocarbon groups by carbon atom number in desulfurized Jet A-1. Reproduced from ref. 12 with permission. Copyright 2015, Elsevier

Carbon atom number	Cycloalkanes C_nH_{2n}	Aromatic hydrocarbons C_nH_{2n-6}	Iso-alkanes C_nH_{2n+2}	*n*-Alkanes C_nH_{2n+2}	Overall content
6	0.0	0.0	0.0	0.0	0.0
7	0.2	0.2	0.0	0.0	0.4
8	1.5	4.5	0.3	1.1	7.3
9	7.8	10.9	1.4	6.3	26.4
10	8.7	4.3	13.0	8.9	35.0
11	2.1	2.5	3.7	5.9	14.1
12	0.4	0.7	1.3	2.8	5.2
13	0.1	0.2	0.9	1.4	2.6
14	0.0	0.0	0.4	0.7	1.1
15	0.0	0.0	0.1	0.3	0.4
16	0.0	0.0	0.0	0.1	0.1
17	0.0	0.0	0.0	0.1	0.1
18	0.0	0.0	0.0	0.0	0.0
wt% sum identified	21.2	23.2	21.2	27.6	92.6
wt% sum corrected	24.9	23.2	24.9	27.6	100.0

cloalkanes. For example, when the carbon ring number exceeds 3, the density of the fuel exceeds 0.90 g mL^{-1}, but the freezing point and viscosity will also both significantly increase, which is not conducive to use at low temperatures for aviation aircraft. Moreover, when the carbon number exceeds 20, the boiling point of cycloalkanes may exceed 350 °C.[8] In fact, the final boiling point of the fuel needs to be limited to a maximum temperature of 300 °C to exclude the heavy compound fraction. A very high concentration of polycycloalkanes along with a relatively low paraffin and monocycloalkanes content will contribute to a high boiling point. Hence, the ideal jet-fuel-range cycloalkanes carbon distribution should be C9–C16 when considering multi-factors.

Lignin is the second-most-abundant component of lignocellulose and also is the only renewable energy with an aromatic ring structure in nature (Fig. 2a). Lignin possesses a complex amorphous polymeric structure of phenylpropane subunits randomly linked by C–C and C–O bonds. It should be noted that the complex structure and numerous chemical bonds of real lignin make it difficult to achieve efficient conversion and the mechanism of real lignin conversion is rather complicated. In this regard, studies performed on lignin derivatives as a feedstock have been widely reported, including the development of catalysts and mechanism investigations.

In the early studies, the hydrodeoxygenation (HDO) route, which only considered the cleavage of C–O bonds, was developed for the production of monocycloalkanes. For example, in the HDO of lignin monomers, such as phenol, guaiacol, or lignin dimers, such as diphenyl ether, benzyl phenyl ether, the unit C–O linkages and the side-chain C–O bonds were cleaved and the C=C bonds on the aromatic ring were saturated to generate C6–C9 monocycloalkanes as the final products (Fig. 2a). Similarly, for the HDO of real lignin with remaining C–C bonds, usually C6–C18 monocycloalkanes and polycycloalkanes mixtures were obtained (Fig. 2b). Recently, researchers have focused on the simultaneous C–C and C–O bond cleavages of the lignin structure, which can convert lignin C–C linkage dimers and real lignin into C6–C9 monocycloalkanes. However, as mentioned above, only C9+ monocycloalkanes are considered as good components of jet fuel. This suggests that the C–C cleavage should be restrained in the HDO of C9+ lignin derivatives and real lignin to obtain more ideal jet-fuel-range cycloalkanes.

Beside the direct HDO route, researchers have found that lignin-derived compounds contain active groups such as hydroxyl, aldehyde, and carbonyl groups, which can be used to construct target carbon chain molecules through C–C coupling reactions (hydroxyalkylation/alkylation, aldol condensation, Michael addition, *etc.*) under acid catalysis, followed by HDO to obtain C9–C16 polycycloalkanes as the final products (Fig. 2b). The as-prepared polycycloalkanes presented excellent jet-fuel properties with comparable density, viscosity, lower heating value, freeze point, and flash point to conventional jet fuel.

To date, we can conclude that work on the catalytic HDO and C–C coupling of lignin and its derivatives into renewable jet-fuel-range cycloalkanes has reached an important stage that requires an in-depth review and constructive outlook. Heterogeneous catalysts, especially metal–acid catalysts, have proven to be efficient catalysts both in HDO and C–C coupling processes. It is necessary to summarize the synthesis pathways and provide a greater in-depth understanding of the corresponding catalytic structure–activity relationship.

To the best of our knowledge, while there are several excellent reviews focused on the HDO of lignin and its derivatives into monocycloalkanes,[13–15] few reviews have focused on the C–C coupling of lignin derivatives into polycycloalkanes. Recently, Li *et al.*[16] summarized the production of cycloalkanes based on two strategies: the utilization of biomass platform compounds intrinsically embodying a carbocyclic structure (HDO route) and the creation of a carbocyclic structure from a biomass platform compound *via* chemical reactions (C–C coupling). However, their comprehensive and profound review did not focus on the transformation of lignin and inter-

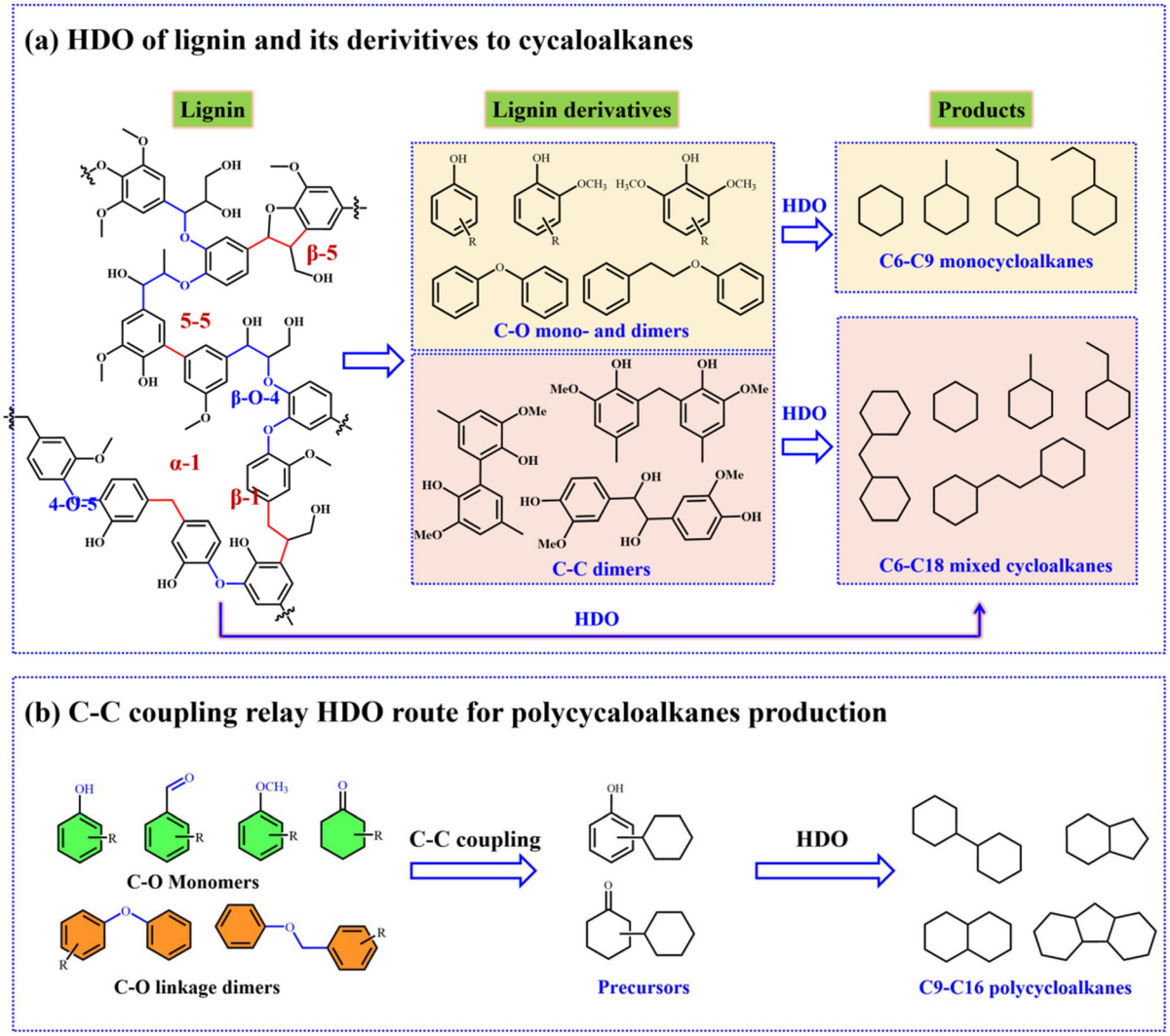

Fig. 2 Schematic of the preparation of cycloalkanes from lignin and its derivatives.

pret the catalytic structure–activity relationship. Therefore, this review focuses on the catalytic HDO and C–C coupling of lignin and its derivatives into renewable jet-fuel-range cycloalkanes over heterogeneous catalysts, with an attempt to systematically summarize the research progress during the past two decades. For the direct HDO route, the catalytic structure–activity relationship is briefly summarized based on the studies on the HDO of lignin derivatives, and then the focus is on the production of jet-fuel-range cycloalkanes by the one-pot conversion of real lignin. Afterwards, the C–C coupling relay HDO route for polycycloalkanes production is emphatically discussed, including the alkylation relay HDO route, aldol condensation relay HDO route, and one-pot conversion route. Finally, based on the systematic summary and comparison of the direct HDO and C–C coupling relay HDO routes, the remaining challenges are highlighted and some perspectives are provided for the future design of structure-specific cycloalkanes. This review may provide insights into the viable utilization of lignin renewable jet-fuel-range cycloalkanes.

2 Direct HDO of lignin and its derivatives into cycloalkanes

Lignin derivatives, including C–O monomers, dimers, and C–C dimers, are usually adopted as feedstock representative of lignin. Ascribed to the intrinsic carbocyclic structure of these lignin derivatives, the HDO route is regarded as the most efficient approach for the production of cycloalkanes. In particular, plenty of studies have focused on the HDO of lignin C–O derivatives (guaiacol, phenol, diphenyl ether, *etc.*) to low-carbon (≤C8) monocycloalkanes. Although these lignin-based low-carbon cycloalkanes are not ideal jet-fuel-range components, knowledge of the catalytic structure–activity relationship of the HDO process based on these studies is insightful and has guiding significance for the further formation of lignin-based C9+ jet fuels. Hence, the HDO of lignin C–O derivatives to monocycloalkanes over metal–acid catalysts is regarded as a model reaction to aid the understanding of the

catalytic structure–activity relationship of the HDO process. In addition, some studies have paid attention to the HDO of lignin C–C dimers, with the production of monocycloalkanes or polycycloalkanes depending on whether C–C cleavage happens. Based on studies on the HDO of lignin derivatives, the simultaneous depolymerization and HDO of real lignin was developed to produce mixtures of cycloalkanes.

2.1. HDO of lignin C–O derivatives to monocycloalkanes over metal–acid catalysts

Generally, highly oxygenophilic metal catalysts with exposed metal sites can first catalyze H_2 dissociation and then mediate C–O cleavage as well as C=C saturation.[17,18] Moreover, it has been reported that the acid sites could promote the hydrolysis of C–O bonds, and the synergism between the metal and acid sites also facilitates the reaction. Therefore, in this part, we summarize the catalytic structure–activity relationship based on regulation of the metal nanostructure, acid property, and synergistic effects during C–O and C–C cleavage over metal–acid catalysts, respectively (Fig. 3).

2.1.1 Reaction route. Scheme 1 shows a schematic diagram of the HDO route for the preparation of monocycloalkanes from guaiacol and diphenyl ether according to previous research, in which guaiacol is regarded as the most typical lignin-derived monomeric model compound. For guaiacol, there are two main HDO routes to form monocycloalkanes as the final product (Scheme 1a). It can be seen that during the HDO to monocycloalkane, the oxygen-containing groups on the side chain are totally removed and the aromatic ring is completely hydrogenated. The C6 ring and the side chain alkyl group are stable without a ring-opening reaction happening. Therefore, After the HDO reaction, the lignin C–O monomers are usually converted into C6–C9 alkylated cyclohexanes, with the original carbon framework remaining unchanged. The HDO of lignin dimers follows the similar rule for monomers, except for cleavage of the C–O linkage between interunits, such as β-O-4, α-O-4, α-O, ad 4-O-5 linkages (Scheme 1b). As a consequence, the lignin C–O dimers with two aromatic rings (C12+ carbon framework) are converted into two pieces of C6–C9 alkylated cyclohexanes.

2.1.2 Catalytic structure–activity relationship

2.1.2.1 Regulation of the metal nanostructure. In most cases, the metal species in the metal–acid catalyst dominate the activity and selectivity in the HDO reaction. The metal nanostructure, including active metal type, particle size, and metal–metal interactions, will significantly determine the adsorption, cleavage, and desorption behaviors of the reactant molecule, including the H_2, substrates, and intermediates.

Noble metals, such as Pt, Pd, and Ru, are widely used as metal sites for bifunctional catalysts in industry because of their excellent hydrogenation function and stability. Compared to non-noble metals, noble metals can catalyze oxygen-con-

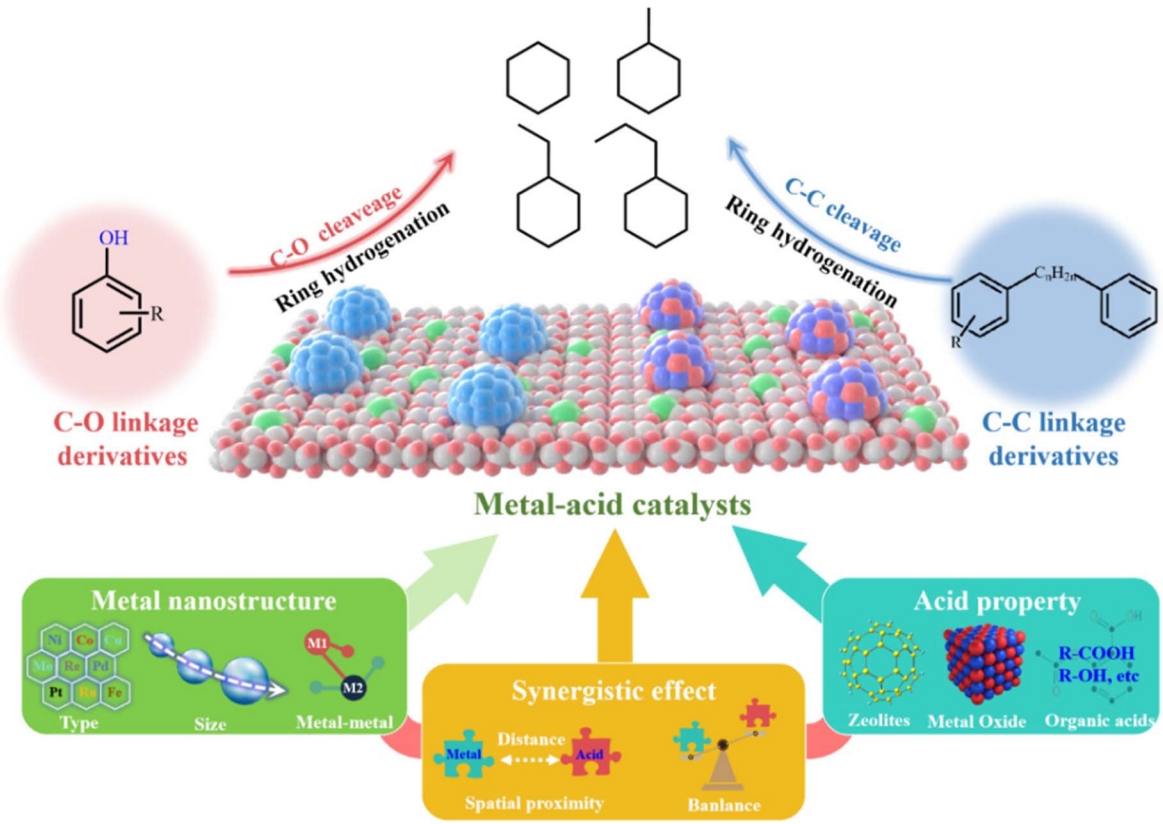

Fig. 3 From lignin derivatives to cycloalkanes: regulatory strategies using metal–acid catalysts.

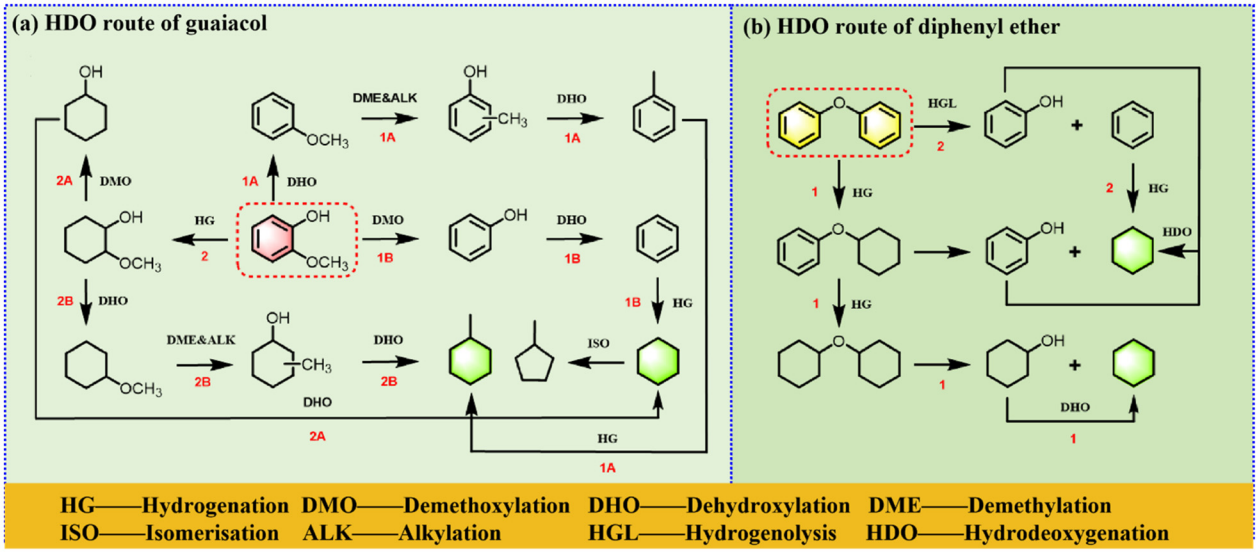

Scheme 1 HDO route of guaiacol and diphenyl ethers to produce monocycloalkanes.

taining compounds effectively in a hydrogen atmosphere under less severe conditions. In the preparation of metal catalysts, improving the metal dispersion on the support is an effective way to promote catalytic efficiency. Compared with metal clusters, isolated metal cations coordinate strongly with the support but weakly to adsorbates, while not being active in the dissociation of H_2.[19] Therefore, the efficiency of the HDO with a single isolated metal may be low. However, dispersing a small amount of isolated metal atoms into another metal to form a bimetallic alloy catalyst can improve the catalytic performance. In addition, the metal particle size is also an important factor affecting the catalytic activity. In general, smaller metal nanoparticles are more favorable for benzene ring hydrogenation.[20] The deactivation rate is also dependent on the particle size, with the smallest Pt size of 1.5 nm showing a high anti-deactivation activity, while larger Pt sizes deactivated faster.[21]

Among many active metals, noble metals can activate H_2 under mild conditions and catalyze the hydrogenation of unsaturated functional groups, thus obtaining higher catalytic performance. However, the scarcity and high price of noble metals hinder their industrial application. As alternatives to noble metals, cheap and readily available transition metals, such as Ni, Co, Fe, and Cu, also exhibit good hydrogenation activity.

Compared with noble metal catalysts, highly dispersed nickel nanoparticles (NNPs) have wider d electron bands, higher energy density, and a stronger activation activity for H_2 and hydrogenated aromatic rings under mild conditions.[22–25] In addition, Ni is less oxygenophilic than other non-noble metals and cannot easily overcome the energy barrier for direct C–O bond cleavage.[26] Therefore, introducing a second active metal can provide new oxygenophilic active sites (*e.g.*, Co, Mo, Fe, W), thus facilitating C–O bond breaking.[27]

Above all, the type of active metal sites significantly affect the hydrogenation performance of the catalysts. In most cases, the hydrogenation ability of noble metals is better than that of non-noble metals. However, to improve the deoxygenation performance, noble metals need to be doped with oxygenophilic metals or combined with acidic sites. This modulation method is also common in the design of non-metal catalysts. This is because the introduction of a second metal increases the oxygen vacancies and improves the dispersion of the metal to some extent. In addition to this, the particle size of the metal and the physical properties of the catalyst are also important factors. For example, in transition-metal phosphides, the synthesis of catalysts with larger specific surface areas and smaller and highly dispersed metal sites facilitates the exposure of more active sites as well as the adsorption and activation of H_2. As for transition-metal sulfides, the reaction performance can be improved by increasing the number of MoS_2 edges.

2.1.2.2 Regulation of the acid properties. It is well known that the acid is the key active site for C–O bond cleavage. Generally, there are two types of acids: Brønsted acids and Lewis acids. The catalytic effect of the acid is inevitably related to the amount and strength of the acid. In this section, the catalytic role of acids in bifunctional catalysis is summarized by the types of different acid supports.

Zeolite acid supports

Aluminosilicate zeolites are widely used as catalysts in the petroleum and refining industries because of the abundance of Brønsted acid sites (Si–OH–Al) in their framework, which can facilitate many reactions.[28] In addition, their shape selectivity is promising for synthesizing target products for different substrates due to the large surface area and ordered pore structure of aluminosilicate zeolites. Typical acidic zeolites include H-Beta, HZSM-5, HUSY, BEA, and MCM-41. The zeolite's pore

structure and acid site strength/concentration are key factors affecting the catalytic activity.

Higher concentrations of acid sites have been reported to favor the formation of carbonium ions, which contribute to dehydroxylation and demethoxylation.[29,30] Catalysts with mesoporous structures and higher concentrations of Brønsted acid sites have better HDO activity for lignin phenolics.[31] Strong acidic sites facilitate dehydration, while weak acid sites adsorb the oxygen atoms in hydroxyl or methoxy groups and improve the cleavage ability of C–O bonds.[32] However, acidity is not the main reason for the catalytic activity. Too large a pore size and strong acidity can lead to coupling reactions and reduce the selectivity for monocycloalkanes. Therefore, the pore-size structure and acidic sites of zeolites need to be regulated rationally.

Metal oxide supports

The structure of metal oxides consists of positive metal ions (cations) with Lewis acids and negative oxygen ions (anions) with Brønsted bases.[33] The metal oxides commonly used in lignin catalytic conversion include Al_2O_3, SiO_2, Nb_2O_5, TiO_2, and ZrO_2. Among these, the unique textural properties of Al_2O_3, such as high surface area, moderate pore-size distribution, suitable acid/base characteristics, and high hydrothermal stability, make it an excellent catalyst support.[34] Moreover, the presence of temperature-stable Lewis acid sites in Al_2O_3 can catalyze the cleavage of ether bonds[35] and the removal of methoxy,[36] which is beneficial for the depolymerization of lignin into monomers.[37] SiO_2, an inert material with excellent hydrothermal stability, has also been used as a catalyst support in the HDO of phenolic compounds.[38,39] Although SiO_2 has poor acid functionality and inactive dehydration properties, it has a large specific surface area and strong adsorption, so other metal oxides with acidic sites can be added to form mixed acidic supports with a large specific surface area and large pore size, such as SiO_2–Al_2O_3,[40] ZrO_2–SiO_2.[41]

In short, weakly acidic metal oxides can be mixed with other acid-strength metal oxides to form mixed supports with a large specific surface area and pore size. Metal oxides with a particular acidic strength can be prepared by changing the preparation method to optimize the morphological characteristics of the supports, thus improving the catalytic activity and stability.

Other acid supports

In addition to zeolites and metal oxides, there are many other acidic functions, such as organic acids. Also, the modification of loaded metal catalysts with organic ligands is a way to modulate the physicochemical properties of catalysts to improve their catalytic performance.[42–44]

Chen *et al.*[45] used an organic ligand with hydrothermal stability, *i.e.*, 4-trifluoromethyl salicylic acid (TFMSA), to modify Ru/γ-Al_2O_3 for the catalytic conversion of lignin phenolic compounds to jet fuel. It was shown that adding TFMSA to Ru/γ-Al_2O_3 helped improve the dispersion of metal nanoparticles, change the ratio of Brønsted/Lewis acid, and significantly increase the amount of Brønsted acid.

In the HDO conversion of phenol, the cyclohexanol hydrogenation rate is much higher than the dehydration rate, indicating that acid-catalyzed cyclohexanol dehydration is the rate-limiting step. Therefore, adjusting the metal and acidactive sites at the bifunctional catalyst interface is crucial to improve the dehydration efficiency. On bifunctional catalysts, the cyclohexanol generated at the metal site can be immediately dehydrated at the nearby acidic site. In contrast, cyclohexanol must repeatedly diffuse between the separated metal and acidic sites on conventional bifunctional catalysts, resulting in a relatively low catalytic activity.

The Brønsted acid site contributes to the dehydration reaction during catalysis, and in some cases, Lewis acids can exhibit better catalysis than Brønsted acids. Lewis acids can selectively bind to and activate specific functional groups (*e.g.*, ether bonds and hydroxyl groups) during the conversion process.[46] For example, metal triflates with strong Lewis acids could effectively catalyze the cleavage of lignin β-O-4 ether bonds.[47]

In summary, acid sites play an important role in removing oxygen from oxygen-containing compounds and facilitating hydrocarbon production. The type and number of acid functions vary slightly from one acid support to another. A reasonable Brønsted/Lewis acid ratio can be obtained by modulation. Brønsted acids offer the more prominent cleavage of C–O bonds than Lewis acids. However, the degree of increase in the strength and the number of acid sites needs to be moderate.

2.1.2.3 Regulation of the metal–acid synergistic effect. We analyzed the roles of the metal and acid sites separately, but a bifunctional catalyst relies on the synergistic interaction between the metal and acid, which has a crucial impact on the catalytic performance.[48] The relationship between the metal and acid is summarized as the "intimacy criterion", proposed by Weisz in 1962. It states that there is a maximum distance between the acid and metal sites beyond which the catalytic activity and selectivity decrease.[49] This criterion has led to the general agreement that in bifunctional catalysts, close contact of the active sites facilitates efficient metal–acid site synergy and a high HDO efficiency.[50] However, Zecevic *et al.*[51] reported a contrary conclusion stating that in bifunctional catalysts, the optimal location of the metal for hydrocarbon conversion is not in the micropores of the zeolite but rather in the surface/mesopores of the zeolite.

Ju *et al.*[56] obtained a highly stable bifunctional catalyst based on Pt-A/Z by the selective deposition of Pt on alumina in an Al_2O_3-ZSM-5 nanocomposite. Shifting the metal–acid distance from the millimeter to nanometer scale improved the catalytic performance for the HDO of eugenol. However, further shortening the distance between the acidic and metal sites did not improve the catalytic performance. Therefore, the generally accepted "closer is better" criterion for metal/acid bifunctional catalysts has some distance limitation in the HDO of bio-oxygenated compounds.

In general, it is more beneficial to improve the catalytic performance when the distance between the metal and the acid site is on the nanometer scale.[57,58] The zeolite encapsulation

approach can shorten the active site spacing and thus improve the catalytic performance because of the synergistic effect between the active sites.[59]

In summary, in the metal–acid-catalyzed HDO system, it is the metal nanostructure (including the active metal type, particle size, and metal–metal interactions), acid property (including the amount and strength of the acid), and synergistic effects (including the ratio balance and spatial proximity) that determine the catalytic activity for the production of monocycloalkanes. Table 2 summarizes the state-of-the-art metal–acid catalysts in the HDO of lignin derivatives to monocycloalkanes. It can be seen that zeolite-supported noble metal catalysts are the most promising options, offering high HDO activity under mild conditions. The efficient HDO progress plays a crucial role not only in the direct HDO of lignin derivatives, but also has great significance in the cascaded HDO of C–C coupling precursors. Therefore, understanding the catalytic structure–activity relationship of the HDO is essential for both the HDO route and C–C coupling route.

2.2 HDO of lignin C–C dimers to cycloalkanes

2.2.1 HDO of lignin C–C dimers with C–C cleavage to produce monocycloalkanes. Compared to the C–O bond (BDE = 209–348 kJ mol^{-1}), the dissociation enthalpy of the C–C bond is significantly higher (BDE = 226–494 kJ mol^{-1}). Until now, relatively little research has focused on lignin C–C bond cleavage, demonstrating that research is still in the initial stage and challenges remain. Researchers have found that zeolites containing Brønsted acid sites can catalyze the cleavage of C–C bonds in petroleum refineries, while these materials alone have poor activity in cleaving C–O bonds in lignin. Therefore, designing and synthesizing bifunctional catalysts with both metal and Brønsted acid sites can theoretically achieve the simultaneous cleavage of lignin C–C and C–O bonds. Some excellent catalysts have been reported, mostly focusing on interunit C–C cleavage to improve the monomer yield,[60,61] but few studies have been able to achieve simultaneous C–C and C–O cleavage and benzene ring hydrogenation to produce monocycloalkane as final products. Dong *et al.*[42] reported a new multifunctional Ru/$NbOPO_4$ catalyst, which integrated Brønsted acid sites onto an emerging NbOx support, coupled with the moderate hydrogenation ability of Ru centers, to enable the cleavage of interunit C–C linkages. Luo *et al.*[62] reported a bifunctional metal molecular sieve Pt/H-MOR catalyst that achieved the pre-activation and selective cleavage of C–C bonds. Overall, for the production of jet-fuel-range cycloalkanes, cleavage of the C–C linkage was not the reaction we were expecting.

2.2.2 Direct HDO of lignin C–C dimers without C–C cleavage to produce polycycloalkanes. Structurally, typical lignin C–C dimers consist of a benzene ring, interunit C–C linkages, and side-chain oxygen-containing groups. For the production polycycloalkanes, it is necessary to achieve the removal of oxygen and benzene ring hydrogenation, and restrain interunit C–C cleavage. In most cases, it is too difficult to cleave the interunit C–C, as stated above. Theoretically, catalysts with excellent HDO activity in the HDO of lignin C–O monomers to monocycloalkanes should be also applied to the HDO of lignin C–C dimers to polycycloalkanes. However, different from lignin C–O derivatives, lignin C–C dimers are not regarded as conventional lignin platform molecules. Thus, scant studies have reported on the direct HDO of lignin C–C dimers to produce polycycloalkanes. Wang *et al.*[63] adopted Ru/Al_2O_3 and HY zeolite for the cleavage of C–O–C bonds without disrupting the C–C linkages in the lignin C–C dimers (β–β, β-5, and 5–5 linkages), which led to the formation of C12–C18 polycyclohexanes.

2.3 One-pot conversion of real lignin to cycloalkanes

Lignin, replete with aromatic ring structures, has demonstrated proficiency as an exceptional substrate in the one-pot synthesis of cycloalkanes *via* hydrodepolymerization. Considering the existence of interunit C–O and C–C linkages, two conversion routes were reported to produce mono/polycy-

Table 2 Overview of the HDO performance of some metal–acid catalysts for the production of monocycloalkanes[a]

Entry	Substrate	Conv. (%)	Catalyst	T (°C)	P (MPa)	t (h)	Solvent	Products	Molar yield (%)	Ref.
1	Diphenyl ether	100	$Ru_{5\%}$/HZSM-5	210	1	2	*n*-Hexane	Cycloalkane	100.0	32
2	Diphenyl ether	100	Ru/Ga-HZSM-5	180	1	2	*n*-Hexane	Cycloalkane	100.0	52
4	Guaiacol	100	5Ni–5Co/NbOx	300	3	2	Dodecane	Cycloalkane	98.9	27
5	Guaiacol	100	Fe(24)Ni(6)–ZrO_2	300	4	8	Octane	Cycloalkane	89.4	53
9	Guaiacol	100	$Ru_{2\%}$/BEA-12.5	250	4	2	—	Cycloalkane	71.9	31
10	Guaiacol	100	Co-Al_2O_3@USY	180	3	4	*n*-Hexane	Cycloalkane	93.6	48
11	Guaiacol	>99	Ru–Cu/HY	250	4	2	H_2O	Cycloalkane	44.8	54
13	Diphenyl ether	100	Ru/SHZSM-5–100	150	1	2	*n*-Hexane	Cycloalkane	100.0	18
14	Guaiacol	100	Ni/ZrO_2–SiO_2	300	5	—	Dodecane	Cycloalkane	96.8	41
15	Guaiacol	100	Ru/TiO_2(TNP)	250	1	4	Octane	Cycloalkane	100.0	55
16	Phenol	100	Ru-20TFMSA/γ-Al_2O_3	240	2	1	Dodecane	Cycloalkane	84.0	45
17	Guaiacol	99.9	Ru/C-HPW	200	1	4	Octane	Cycloalkane	98.6	50
18	Eugenol	77.3	Pt-A/Z	300	4	4	*n*-Hexane	Propylcycloalkane	38.0	56
19	Phenol	100	Ru@H-ZSM-5	150	5	4	Decalin	Cycloalkane	90.0	57
20	Guaiacol	100	Ru@HMCM-22-IN	160	3	5	Dodecane	Cycloalkane	>95.0	58

[a] The molar yield of monocycloalkane was calculated based on the C6 ring molar of initial substrate and product.

cloalkanes mixtures and monocycloalkanes, respectively. The first route only involved the cleavage of C–O linkages, whereas the C–C linkages remained, leading to the formation of mono/polycycloalkane mixtures as the final products. The second route involved the simultaneous cleavage of C–O and C–C linkages, leading only to monocycloalkanes as the main products. Both routes were significantly influenced by the structure property of lignin and the catalytic system.

2.3.1 Production of mono- and polycycloalkanes mixtures *via* the cleavage of C–O linkages. Similar to the HDO of lignin C–O derivatives to monocycloalkanes, the one-pot hydrodepolymerization of real lignin to mono- and polycycloalkanes mixtures has been extensively studied. Typical metal–acid catalyst with Ru, Pt, Ni, Re, *etc.* as metal sites, and C, zeolites, Nb_2O_5, *etc.*, as acid supports have been proven to be efficient in the selective hydrodepolymerization of real lignin into mono- and polycycloalkanes mixtures.[54,64–67] Table 3 displays the bond dissociation energy of common C–O and C–C linkages and their approximate abundance in softwood and hardwood lignin.[42] It can be inferred that lignin with more abundant C–C linkages would lead to a lower monocycloalkane yield if the C–C linkages remained intact. Moreover, the higher dissociation energy of C–C bonds makes them more challenging to break compared with C–O bonds. Hence, in most cases, the hydrodepolymerization of real lignin over metal–acid catalysts results in mono- and polycycloalkanes mixtures as the final products.

Most studies only demonstrated the production of cycloalkanes as bio-fuels or bulk chemicals, but did not investigate their properties. As for lignin-based jet fuel, it should meet the current ASTM D7566 standard specifications.[68] Fig. 4a illustrates the proposed processing pathway for converting lignin to jet-fuel-range C9+ mono- and polycycloalkanes.[69] However, the formation of light hydrocarbons (≤C8) cannot be avoided and sometimes they exist as main products, as shown in Table 4. Recently, researchers have paid more attention to the chemical compositions and properties of lignin-based jet-fuel-range hydrocarbons. Prof. Yang *et al.*[8] adopted comprehensive

Table 3 Bond dissociation energy of common C–O and C–C linkages and approximate abundance in softwood and hardwood lignin. Reproduced from Ref. 42. with permission. Copyright 2019, Cellpress

Linkage		Bond dissociation energy/kJ mol^{-1}	Number/100 ppu		
			Softwood	Hardwood	Grasses
C–O bonds	β-O-4	226–301	43–50	50–65	74–84
	α-O-4	209–234	6–8	4–8	5–11
	4-O-5	327–348	4	6–7	n.d.
	5–5	481–494	10–25	4–10	n.d.
C–C bonds	β-5	226–264	9–12	4–6	5–11
	β–β	281–339	2–4	3–7	1–7
	β-1	272–289	3–7	5–7	n.d.

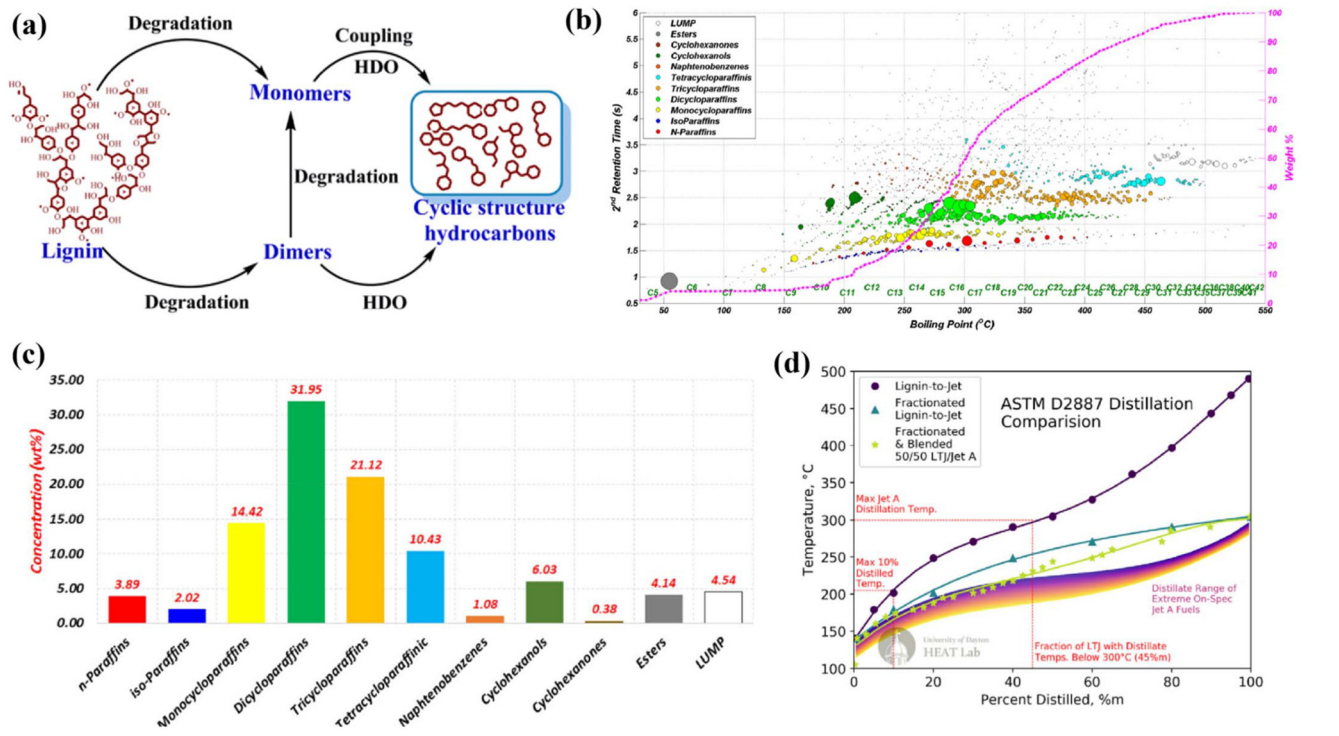

Fig. 4 (a) Proposed processing pathway for converting lignin into jet fuel. Reproduced from ref. 69 with permission. Copyright 2018, the American Institute of Aeronautics and Astronautics, Inc. (b) Bubble plot representation of a 'normal' GC × GC-FID contour plot for the sample; (c) summary of the GC × GC-FID hydrocarbon composition (wt%); (d) simulated distillation curves of lignin jet fuel compared to some reference jet fuels. Reproduced from ref. 8 with permission. Copyright 2019, Elsevier.

Table 4 One-pot hydrodepolymerization of real lignin to cycloalkanes over different catalysts[a]

Entry	Substrate	Catalyst	T (°C)	P (MPa)	t (h)	Products	Yield (wt%)	Ref.
1	Birch lignin	Ru/C	250	0.7	20	Monocycloalkanes	29.3	64
2	Pyrolysis bio-oil from pinewood	RANEY® Ni + H-BEA-35	160	2-PrOH	2	Cycloalkanes	7.2	71
3	Birch lignin	$Ru/NbOPO_4$	310	5	40	C6–C9 cycloalkanes	12.0	42
4	Poplar lignin	$Mo_{0.06}$–Co_9S_8/Al_2O_3	265	3	20	Monocycloalkanes	5.6	72
5	Pyrolysis bio-oil from poplar wood	Ni/Nb_2O_5	300	7	16	Cycloalkanes	25.4	66
6	Kraft lignin	S–NiMo/MgO–La_2O_3	350	10	4	Cycloalkanes	1.1	67
7	Organosolv lignin	Ir–$ReOx/SiO_2$	260	4	10	Monocycloalkanes	19.5	67
						Polycycloalkanes	1.6	
8	Birch lignin	$Pt/NbOPO_4$	190	5	20	Alkylcyclohexanes	4.8	65
9	Enzymatic lignin	Ni/ASA-1	300	6	160 min	Monocycloalkanes	35.3	73
						Polycycloalkanes	6.1	
10	Lignin	Ni/S-1	300	6	2	C6–C9 cycloalkanes	24.0	74
						C10–C17 cycloalkanes	9.0	
11	Organosolv lignin	Pt/HAP + Ni/ASA	300	6	4.5	Monocycloalkanes	26.5	75
						Polycycloalkanes	15.5	
12	Organosolv lignin	Ni/HBEA	250	2	6	Monocycloalkanes	29.1	76
						Polycycloalkanes	6.0	
13	Poplar lignin	Ni_2P–Al_2O_3(H)71	250	5	15	Monocycloalkanes	6.0	77
						Polycycloalkanes	1.0	
14	Pine wood lignin	RuNi/HY	250	4	4	Hydrocarbon products	32.0	54
15	Dimers of pine sawdust	Pd/C	300	3	16	C16–C18 cycloalkanes	28.0	78
16	Alkali lignin	HY + Ru/Al_2O_3	300	4	4	C7–C11 cycloalkanes	3.4	63
						C12–C18 cycloalkanes	18.4	
17	Pyrolysis bio-oil from eucalyptus wood	Pd/*m*-MoO_3–P_2O_5/SiO_2	250	1	15	C6–C9 cycloalkanes	13.4	79
18	Birch lignin	Pd/Nb_2O_5	250	0.7	20	C7–C9 cycloalkanes	24.4	80
19	Oligomer of hardwood	Pt/H-MOR	300	4	24	C6–C9 cycloalkanes	36.8	62

[a] Calculation of the product mass yield was based on the masses of the initial lignin reactant and final products.

two-dimensional gas chromatography (GC × GC) with both mass spectrometry and flame ionization (FID) detection to identify and quantify the species in lignin-based jet fuel (US patent 9518076 B2). As shown in Fig. 4b, the main compositions were *n*-paraffins, iso-paraffins, and mono-, di-, and tricycloalkanes, of which the majority contained carbon numbers in the range of 7–20. Among them, cycloalkanes were the most abundant components with the concentrations of mono-, di-, tri-, and tetra-cycloalkanes being 14.42, 31.95, 21.12, and 10.43 wt%, respectively (Fig. 4c). Fig. 4d presents a comparison of the simulated distillation (SimDis) (ASTM D2887) data of lignin-based jet fuel, a fractionated lignin-based jet fuel, a fractionated and 50/50 wt% blend with conventional jet fuel, and a range of jet fuels with extreme operability properties. The result showed that the neat lignin-based jet fuel could hardly meet the standard of jet fuel. It is therefore usually blended with conventional jet fuel, with a strict blend limit (<10 wt%). Further, Prof. Yang *et al.*[70] removed 10% of C6 monocycloalkanes and C17+ molecules from lignin-based jet fuel in an attempt to achieve a higher blending ratio with conventional jet fuel. As mentioned above, removing the C17+ molecules should improve the low-temperature viscosity and freezing point of the neat LJF sample, while removing the C6 cyclohexane will retain the flash point above the specification limit. The results also proved that the blend limit could be improved to 20% after the removal. Their latest research also claimed that an elevated concentration of C7 and C8 will lead to a violation of the flash point, and these components should be removed by distillation.[7]

To sum up, real lignin can be converted into mono- and polycycloalkanes mixtures *via* a simultaneous depolymerization and HDO, and so-called lignin-based jet fuel with carbon numbers in the range of C6–C20 could be obtained. This lignin-based jet fuel still has some distance to meet the current jet fuel standards due to the inevitably generated light cycloalkanes (≤C8) and C17+ polycycloalkanes. The high concentration of light cycloalkanes and C17+ polycycloalkanes will contribute to violations of the flash point and boiling point limits, respectively. More studies should be performed on the after treatment of lignin-based jet fuel to meet the ASTM standard.

2.3.2 Production of monocycloalkanes *via* the simultaneous cleavage of C–C and C–O linkages. The existence of large molecule fragments or oligomers with interunit C–C bonds during the depolymerization of real lignin significantly limits the production of monocycloalkanes, but the cleavage of intrinsic C–C bonds remains a long-standing challenge. To date, few studies have focused on the production of monocycloalkanes *via* the simultaneous cleavage of C–O and C–C linkages. Dong *et al.*[42] developed a $Ru/NbOPO_4$ catalyst to break the 5–5 bond in 2,2′-biphenols, resulting in breaking yields of monobenzene and monocycloalkane, which were 1.2–1.5 times the yields obtained from the established nitrobenzene oxidation method. Recently, Luo *et al.*[62] designed a Pt/H-MOR catalyst with the synergistic action between the Pt (de)hydrogenation function and Brønsted acid sites confined in the micropores of the H-MOR zeolite, to strengthen the selectively cleavage of C–C and C–O linkages as well as the complete

hydrogenation, leading to an extremely high yield of monocycloalkanes. These excellent studies reported substantially improved monomer yields, and made great contributions to the scission of various C–C bonds. However, monocycloalkanes, especially light cycloalkanes (≤C8), are not ideal jet-fuel components.

3 C–C coupling relay HDO route to produce polycycloalkanes

Compared with most monocycloalkanes, polycycloalkanes are denser and more suitable for high-density jet fuel. Among them, bicyclohexane has been extensively studied as a component of jet fuel.[81] This is because the density of bicyclohexane is about 0.887 g mL^{-1}, which is higher than that of the conventional jet fuel RP-3 (0.783 g mL^{-1}, 15 °C).[82] Typically, bicyclohexane is synthesized by the hydrogenation of biphenyls[83] or dibenzofurans[84] isolated from petroleum. Recently, as a critical high-density biofuel, it was reported that bicyclohexane could also be produced from lignin-based compounds. The synthesis of bicyclohexane involves two steps, namely, synthesis of the bicyclohexane precursor followed by HDO. Bicyclohexane precursors can be synthesized from cyclohexanone's aldol condensation or phenol's alkylation with alcohol. Phenol, a classical platform compound from lignin hydrolysis, can be selectively hydrogenated to obtain cyclohexanone/cyclohexanol, followed by a C–C coupling reaction.

Although the density of bicyclohexane is high, the freezing point value (2.6 °C) needs to be reduced but it can be used as a fuel additive (Table 5). In contrast, polycycloalkanes containing a five-membered ring structure, such as cyclopentyl, cyclohexane, and (cyclopentyl methyl)cyclohexane, have good low-temperature properties due to their asymmetric structure. Such substances can be obtained either by alkylation reactions of cyclopentanol and lignin phenolic compounds[85] or by promoting isomerization reactions during the HDO of lignin phenolic compounds.[86] In addition, decahydronaphthalene has been widely researched as an aviation fuel additive with a high thermal stability and energy density. Decahydronaphthalene is mainly obtained from the hydrogenation of naphthalene in petroleum. In the long term, there is still a need to develop renewable synthetic routes for decahydronaphthalene. Structurally, decahydronaphthalene consists of two cyclohexanes, so lignin derivatives with a six-membered ring structure can be used as raw materials for the preparation of decahydronaphthalene. Generally, besides the strategy involving the direct HDO of lignin C–C dimers or multimers intrinsically embodying a multi-carbocyclic structure without C–C cleavage, another strategy involves the creation of a multi-carbocyclic structure *via* the C–C coupling of lignin C–O derivatives followed by HDO. The catalysis system, including reaction route, catalysts, mechanism, presents significant differences based on the different detailed reactions. In this chapter, we start with the design thoughts on the reaction route, and then emphatically discuss the corresponding catalytic structure–activity relationship.

Unlike lignin C–C dimers, lignin C–O derivatives first require C–C coupling to form dimer precursors with a multi-carbocyclic structure, followed by the HDO reaction to produce polycycloalkanes. According to the different structures of various lignin C–O derivatives, mainly three C–C coupling routes have been designed to synthesize multi-carbocyclic precursors, including the alkylation relay HDO route, aldol condensation relay HDO route, and one-pot conversion (Fig. 5).

3.1 Alkylation relay HDO route for polycycloalkanes production

As illustrated in Fig. 5a, the alkylation reaction route is suitable for the C–C coupling of lignin-derived phenols and ethers with the existence of an alkylation reagent. The reaction pathway generally follows the following steps: (1) The alkylation reagent produces carbonium ions in a transition state under the catalysis of acid catalyst A, and then replaces the active hydrogen on the benzene ring of the lignin C–O derivatives to generate a multi-carbocyclic precursor; during this step, the lignin-derived phenols or ethers with the original single-carbocyclic framework are transformed into dimers with a multi-carbocyclic framework *via* C–C coupling; (2) the precursor further undergoes HDO over catalyst B to finally produce polycycloalkanes; during this step, the oxygen-containing groups are removed and the carbon rings become saturated, with the multi-carbocyclic framework unchanged. The commonly used alkylation reagents include cycloalcohols and benzyl alcohols, while the commonly used acid catalysts

Table 5 Fuel properties of typical polycycloalkanes

Entry	Compounds	Density (g mL^{-1}, 20 °C)	Freezing point (°C)	Viscosity (mm^2 s^{-1}, 20 °C)	Ref.
1	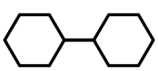	0.887	2.6	4.5	81
2	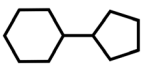	0.88	<75	2.0	85
3	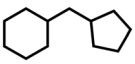	0.87	<−80	2.9	87
4		0.88	<−30	2.3 (37.8 °C)	88–90

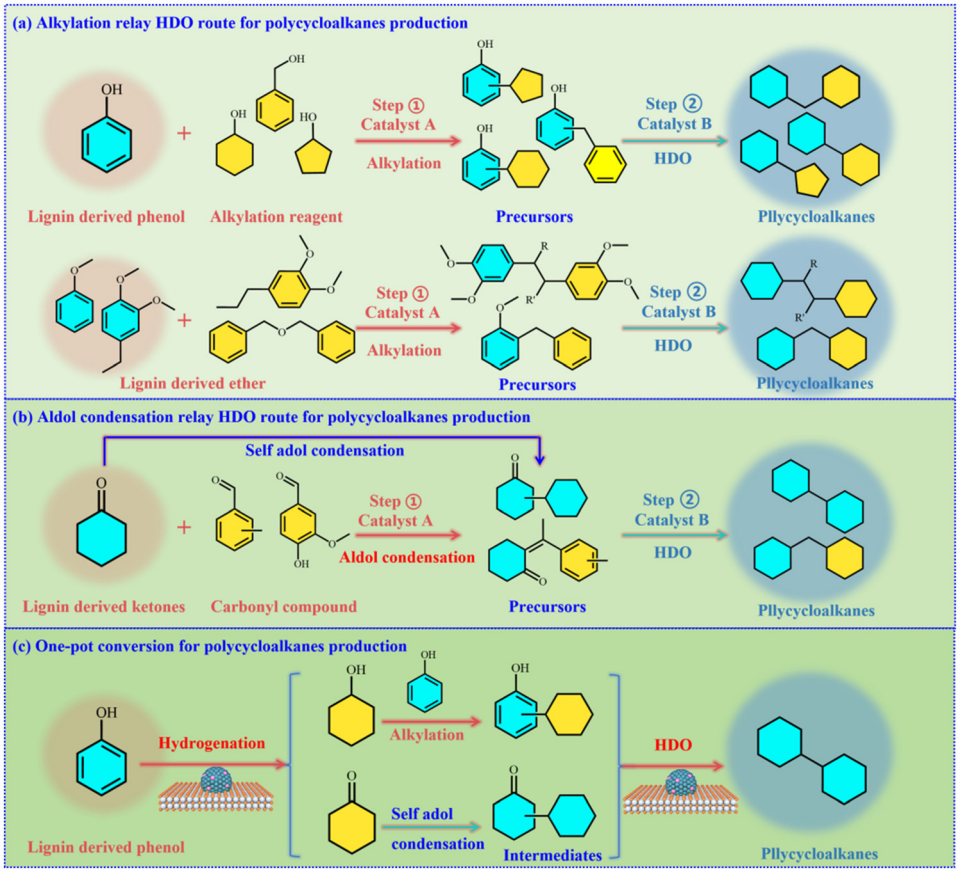

Fig. 5 Reaction routes for converting lignin derivatives into polycycloalkane. (a) Alkylation relay HDO route, (b) aldol condensation relay HDO route, (c) one-pot conversion route.

include acidic zeolites (HUSY, HBEA, Al-SBA-15, HY), acidic resins, and heteropolyacids.

Nie *et al.*[91] investigated the alkylation reaction of phenol with cyclopentanol catalyzed by hydrophobic acid resin (R-*x*) under mild conditions (140 °C for 4 h). Among the catalytic results for R-*x* (*x* = 0.25–1.5), R-0.25 (79.8% phenol conversion) was much better than Hβ (51.6% phenol conversion), mainly due to the more acidic and better hydrophobic nature of R-*x* than Hβ. In bifunctional catalysts, the acid site also has the function of dehydration, which is a competitive reaction with alkylation. Therefore, it is not desirable to excessively pursue the acid site strength, and it is more important to consider how to balance the relationship between excessive dehydration and alkylation. At the same time, extreme acid sites may lead to products with larger molecular weights, which is not favorable for forming the target alkylation products.[92] Therefore, the strength and number of acid sites need to be appropriate.

In addition to the acidity, the solid acid morphology characteristics are important factors that can affecting the product distribution. Large-pore-sized zeolites facilitate the diffusion of macromolecular intermediates, while small-pore-sized supports have spatial hindrances and are not conductive to forming polycycloalkanes.[93] However, the macroporous zeolite produced after excessive alkali treatment causes a partial collapse of the zeolite framework structure, reducing its specific surface area and total acid content.[94] In addition, solid acids with a high specific surface area at appropriate acid amounts and acidity make it easy for the molecules to come into contact with the acid sites.[95]

Zhao *et al.*[96] found that the alkylation of phenol and cyclohexanol was high enough for effective alkylation reactions when the molar ratio of phenol to metal was relatively high. At 473 K, the optimized phenol/Pd ratio was 2254–4508 mol mol^{-1} with a 67%–85% yield of the alkylation products. When the phenol/Pd ratio was reduced to 564 mol mol^{-1}, the dominant product was cyclohexane (98% yield), while the alkylation product accounted for only 2.1%. In addition, Pd/HBEA showed higher selectivity for alkylation than the physically mixed catalyst, indicating that the shorter distance between the metal and acid sites significantly increased the probability of the C–C coupling reaction occurring between the phenol and intermediate. Moreover, strong Brønsted solid acids catalyze dehydration but not C–C bond formation. Only in combination with the pore size of the zeolite pore channel can phenol undergo C–C coupling at the Brønsted acid site and then be hydrodeoxygenated to polycycloalkanes.

Zou's group[95,97] reported the alkylation of benzyl ether (or benzyl alcohols) with phenols, including phenol, anisole, and guaiacol. After the HDO of the alkylation product over the Pd/

C+ HZSM-5 catalyst, polycycloalkanes with a bicyclic structure were obtained. They also synthesized substituted diphenyl methane by the acid-catalytic alkylation of lignin-derived phenols (phenol, anisole, guaiacol) with benzyl ether or benzyl alcohols (Fig. 6).[95] The result showed that among the different solid acid catalysts, MMT-K10 exhibited superior activity than HPW, Amberlyst-15, and Al-MCM41, with 80.6% selectivity for the substituted diphenylmethane precursor, ascribed to its modest acid property and open lamellar structure (Fig. 6a). Besides, the effects of the reactant ratio and type were evaluated to obtain an optimized activity (Fig. 6b and c). They also synthesized ethyl-substituted bicyclic cycloalkanes from the lignin-derived 4-ethylphenol and phenylmethanol.[97] In this alkylation reaction, HPW was found to work as a better catalyst with 71% selectivity for the monoalkylated products (2-benzyl-4-ethylphenol and 3-benzyl-4-ethylphenol) (Fig. 6d and e). The resulting fuel had a density and viscosity of 0.873 g cm^{-3} and 10.7 mm^2 s^{-1}, respectively, at 20 °C. Moreover, the freezing point of the fuel was −42 °C, much lower than that of dicyclohexylmethane and dicyclohexane.

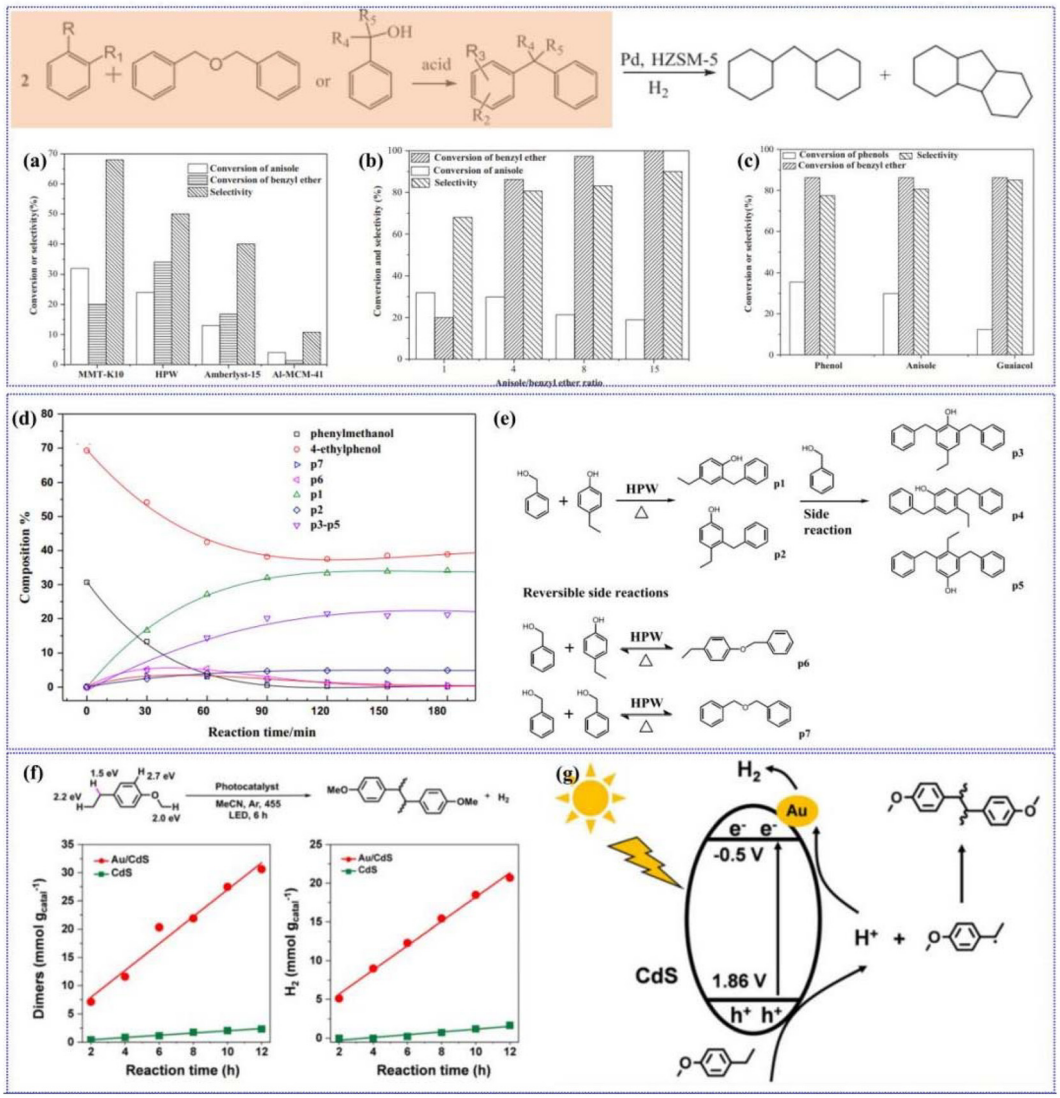

Fig. 6 (a) Performance of catalysts in the alkylation of anisole with benzyl ether over different catalysts. Reaction conditions: 23.3 mmol anisole, 23.3 mmol benzyl ether, 0.1 g catalyst, 110 °C, 2 h. (b) Effect of anisole to benzyl ether ratio in the alkylation reaction over MMT-K10. (c) Alkylation of different phenols with benzyl ether over MMT-K10. Reaction conditions: 23.3 mmol phenols, 5.83 mmol benzyl ether (2.92 mmol for guaiacol), 0.1 g MMT-K10, 110 °C (90 °C for guaiacol), 2 h (9 h for guaiacol). Reproduced from ref. 95 with permission. Copyright 2017, Elsevier. (d) Schematic alkylation reaction of 4-ethylphenol with phenylmethanol. (e) Distribution of substances during the process of the alkylation reaction. Reaction conditions: 9.77 g (80 mmol) 4-ethylphenol, 4.32 g (40 mmol) phenylmethanol, 0.85 wt% HPW, 110 °C. Reproduced from ref. 97 with permission. Copyright 2018, Elsevier. (f) Time-on-course process of the production over Au/CdS and CdS. Reaction conditions: 1 mL of 4-ethyl-1-methoxybenzene, 50 mg of Au/CdS, 10 mL of CH_3CN, 455 nm LED (60 W) irradiation, Ar atmosphere. (g) Proposed reaction mechanism for the photocatalytic dehydrocoupling of 4-ethyl-1-methoxybenzene. Reproduced from ref. 78 with permission, Copyright 2021. Wiley.

Beside thermocatalytic alkylation over an acid catalyst, photocatalytic C–C coupling was also developed for some thermodynamically unfavorable reactions. Dou *et al.*[78] performed the photocatalytic coupling of lignin-derived 4-ethyl-1-methoxybenzene using an Au/CdS photocatalyst under visible-light (455 nm LEDs) irradiation in MeCN solvent at room temperature. The yield of the dimer reached 83 wt% in 24 h accompanied with 11 mmol g_{catal}^{-1} H_2 production (Fig. 6f). The catalyst was also active for the self-coupling of various lignin-derived phenolics to form dimers with 57–83 wt% yields. The proposed reaction mechanism revealed the combination of Au and CdS could significantly improve the separation of photogenerated electrons and holes, which finally enhances the coupling activity of Au/CdS (Fig. 6g).

3.2 Aldol condensation relay HDO route for polycycloalkanes production

Hydroxyaldol condensation is a nucleophilic addition reaction of an aldehyde or ketone with an α hydrogen atom with another carbonyl compound usually catalyzed by an acid or base. This enables not only lignin derivatives bearing $-OCH_3$ or –OH groups but also derivatives encompassing carbonyl groups to achieve ring constitution. Typically, lignin-derived aldehydes and ketones include cyclohexanone, methyl benzaldehyde, and vanillin. In the aldol condensation of lignin-derived aldehydes and ketones, mainly two tactics can be utilized: (1) cross condensation of lignin-derived aldehyde or ketone with another aldehyde or ketone; (2) self-aldol-condensation of cyclohexanone (Fig. 5b). After cascade HDO progress over a metal or metal–acid catalyst, the condensed precursor can be converted into polycycloalkanes. The carbon framework change law is similar to that in the alkylation relay HDO route.

Methyl benzaldehyde and vanillin, typical downstream products obtained *via* the catalytic oxidation of lignin, are usually employed as aldehyde reagents to participate in the cross condensation, while cyclohexanone, cyclopentanone, methyl isobutyl ketone, *etc*. are regarded as ketone reagents. Xu *et al.*[98] reported the synthesis of C14 oxygenates (*i.e.*, 2-(2-methylbenzylidene)cyclohexanone or 2-(4-methylbenzylidene)cyclohexapnone) from the aldol condensation of 2-methyl benzaldehyde (or 4-methyl benzaldehyde) and cyclohexanone (Fig. 7a). Among the investigated catalysts, they found that the EAOAc ionic liquid presented superior activity and good stability, with carbon yields 85% under 353 K for 6 h. The mechanism study showed that the excellent performance of the EAOAc ionic liquid could be ascribed to its special chemical structure and/or the synergetic effect of ethanolamine and acetic acid (Fig. 7b).

Beside acid catalysts, base catalysts can also be used in the aldol condensation. Zhang *et al.*[99] reported the aldol condensation of methyl benzaldehyde and methyl isobutyl ketone to synthesize C–C coupling precursors over solid base catalysts. Interestingly, the as-synthesized precursors could be converted into polycycloalkanes *via* intramolecular dehydration/alkylation/hydrogenation reactions (Fig. 7c). Among the studied solid bases, K_2CO_3/Al_2O_3 showed the highest activity in the aldol condensation reaction, which might be rationalized by its larger base site concentration and higher specific surface area. Moreover, K_2CO_3/Al_2O_3 was effective for the aldol condensation of other ketones, and the as-synthesized precursors could be transformed into octahydro-indenes with different structures (Fig. 7d). The cycloalkane mixtures obtained in this work had a density of 0.857–0.944 g mL^{-1}, higher than the currently used jet fuel (~0.8 g mL^{-1}). In addition, they had freezing points of 227.7–240 K and could be used to improve the volumetric heat values and/or thermal stability of jet fuels.

It is well known that cyclohexanone can be obtained from the hydrogenation reaction of lignin-derived phenol, and it can undergo self-condensation to construct interunit C–C bonds between C6 rings. Liu *et al.*[100] demonstrated that phenol could be selectively hydrogenated to cyclohexanone over a dual supported Pd-Lewis acid catalyst, with both the conversion and selectivity exceeding 99.9%. However, it should be noted that phenol hydrogenation to cyclohexanol was much easier than cyclohexanone. In most cases, the self-condensation of cyclohexanone happened during the one-pot conversion of phenol, which is discussed in the next section. Until now, few studies have been reported on the direct self-condensation of cyclohexanone (employed as an initial reactant) to produce bicyclohexane. Sun *et al.*[101] performed the self-condensation of cyclohexanone over the base-Mg–Zr–O catalyst, with the formation of a bicyclic oxygenate precursor. However, the self-coupling depth was insufficient, and limited the production of larger molecules.

Generally, the condensation between cyclic ketones presents a greater priority than that between cyclic ketones and linear aldehydes or ketones, leading to the production of bicyclic oxygenate precursors of jet fuel with a higher C number. Both acid and base catalysts have been proven to be effective in cross- and self-condensation reactions. In addition, similar to the alkylation relay HDO route, two different catalysts for the cascade reaction are essential in the aldol condensation relay HDO route to achieve polycycloalkanes as the final products (Table 6).

3.3 One-pot conversion

The above-mentioned tandem catalysis of lignin C–O derivatives to polycycloalkanes has been proven to be an effective route, but it needs two steps with two different catalysts in different catalytic systems. Therefore, some advanced studies have attempted the one-pot conversion of lignin C–O derivatives into polycycloalkanes. It was found that phenol, and its hydrogenation products, including cyclohexanol and cyclohexanone, are important reactants during the alkylation and aldol condensation reactions. In detail, the phenol can react with cyclohexanol *via* alkylation to generate cyclohexylphenol as a precursor, and cyclohexanone can convert this to 3-cyclohexanylcyclohexanone as a precursor (Fig. 5c). Considering the subsequent HDO of the bicyclic oxygenate precursor, both metal and acid sites are necessary in the one-pot conversion system.

However, as discussed in Chapter 2, metal–acid catalysts are efficient for the production of monocycloalkanes from lignin C–O derivatives. Scheme 2 displays the reaction pathway comparison for monocycloalkanes and polycycloalkanes production from phenol conversion over metal–acid catalysts. Recently,

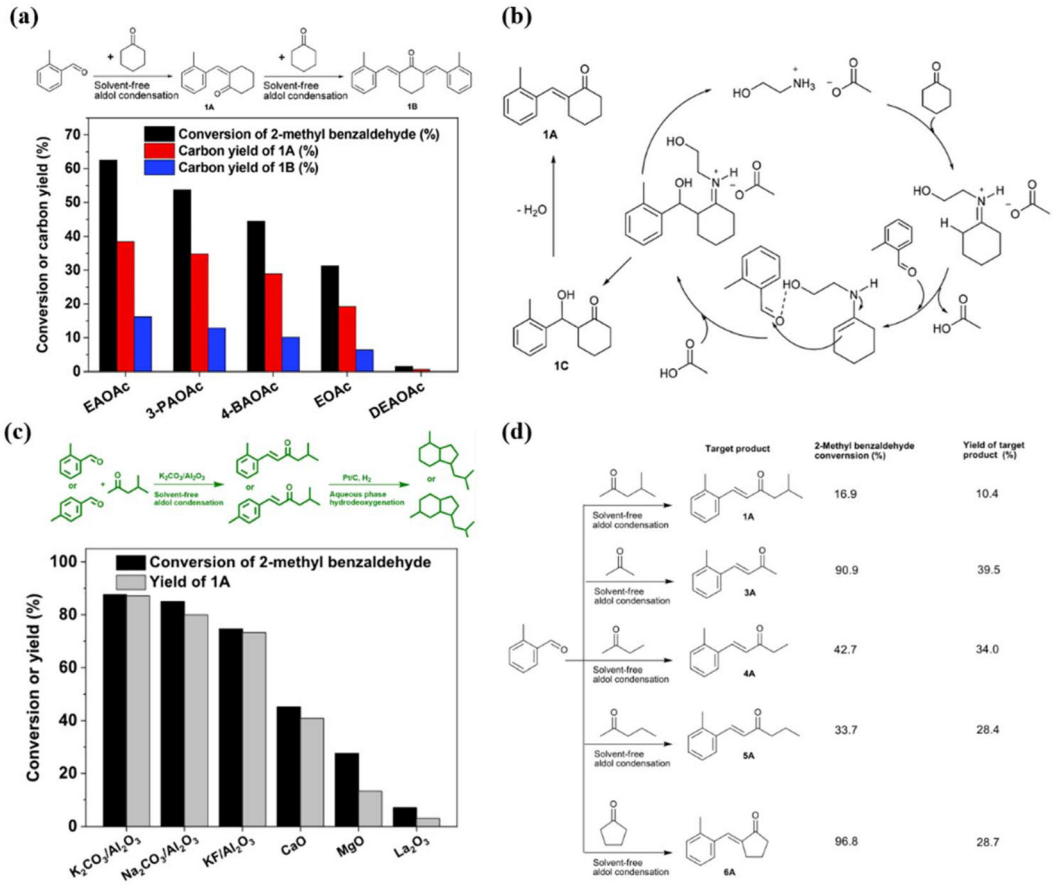

Fig. 7 (a) Conversions of 2-methyl benzaldehyde and the carbon yields of **1A** or **1B** over ionic liquid catalysts. Reaction conditions: 10 mmol 2-methyl benzaldehyde, 10 mmol cyclohexanone, 1 mmol ionic liquid; 333 K, 4 h. (b) Reaction mechanism for the generation of **1A** from the aldol condensation of 2-methyl benzaldehyde and cyclohexanone. Reproduced from ref. 98. with permission, Copyright 2018. Royal Society of Chemistry. (c) 2-Methyl benzaldehyde conversions and **1A** yields over solid bases. Reaction conditions: 10 mmol MIBK, 10 mmol 2-methyl benzaldehyde, 0.2 g catalyst; 403 K, 6 h. (d) Results for the aldol condensation reactions of 2-methyl benzaldehyde with different ketones over K_2CO_3/Al_2O_3. Reaction conditions: 20 mmol ketone, 10 mmol 2-methyl benzaldehyde, 0.2 g catalyst; 353 K, 6 h. Reproduced from ref. 99 with permission, Copyright 2019. American Chemical Society.

Table 6 Overview of the two-step tandem catalysis of lignin C–O derivatives to polycycloalkanes[a]

		C–C coupling			HDO			
Entry	Substrate	Catalyst A	C–C coupling precursor	Molar yield (%)	Catalyst B	Polycycloalkanes	Molar yield (%)	Ref.
1	Cyclopentanone Cyclohexanone	R-2	Bicyclic compounds Tricyclic compounds	~85.0	Pd/Hβ	Bicyclic alkanes Tricyclic alkanes	57.0 41.8	91
2	Phenol Cyclopentanol	Hβ	Bicyclic compounds Tricyclic compounds	52.6 14.3	Pd/C	Bicyclic alkanes Tricyclic alkanes	74.3 16.2	95
3	4-Ethylphenol Phenylmethanol	HPW	2-Benzyl-4-ethylphenol 3-Benzyl-4-ethylphenol	71[b]	Pd/C HZSM-5	Bicyclic alkanes	79.2	97
4	4-Ethyl-1-methoxybenzene	Au/CdS	Dimers	83.0	Pd/C	C16–C18 cyclic alkanes	58.0	78
5	Methyl benzaldehyde Cyclohexanone	EAOAc	2-(2-Methylbenzylidene) cyclohexanone	85.0	Pd/C	1-Methyldodecahydro-1*H*-fluorene	92.5	98
6	Methyl isobutyl ketone Methyl benzaldehyde	K_2CO_3/Al_2O_3	Branched octahydro-indenes	86.2	Pd/C	Branched octahydro-indene	96.8	99

[a] The molar yield of polycycloalkane was calculated based on the C6 ring molar of initial substrate and product. [b] Total selectivity of 2-benzyl-4-ethylphenol and 3-benzyl-4-ethylphenol.

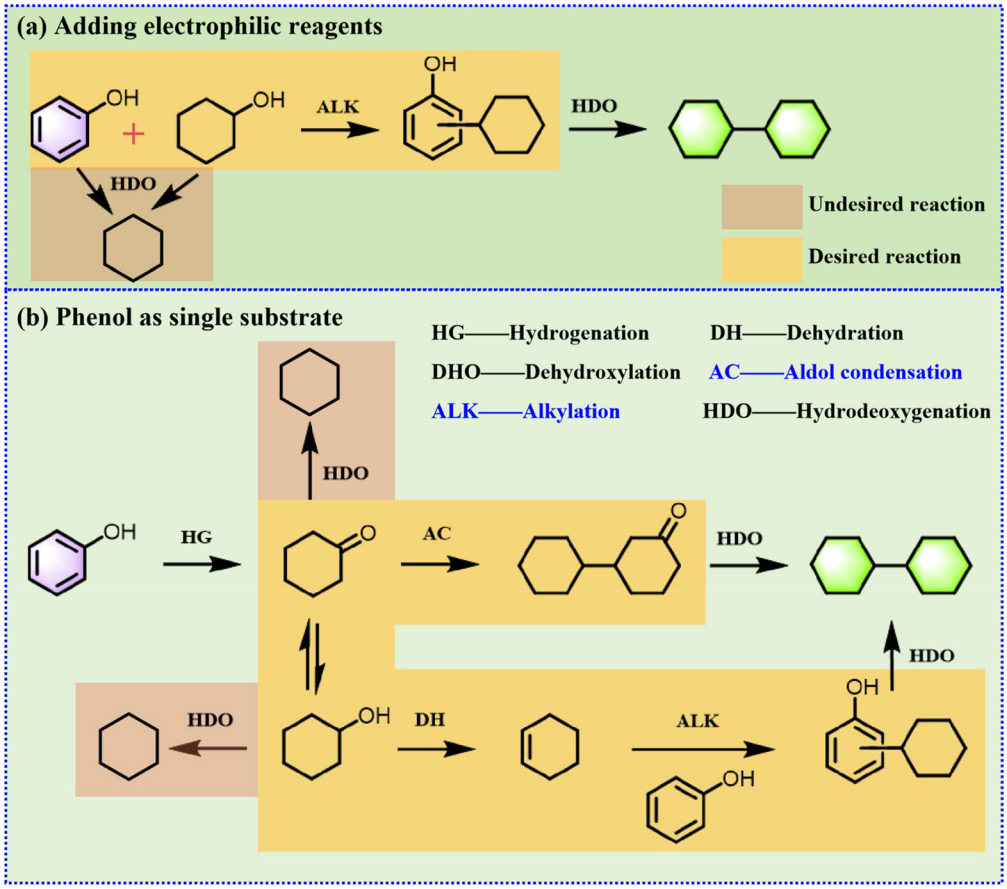

Scheme 2 One-pot reaction pathway comparison for monocycloalkanes and polycycloalkanes production from phenol conversion.

several studies have achieved important progress on the metal–acid-catalyzed one-pot conversion of phenol to polycycloalkane *via* regulating the microstructure of the catalysts and reaction conditions. There are mainly two different synthetic routes: (a) adding cyclohexylphenol or cyclopentanol as electrophilic reagents, which react with phenol *via* alkylation; or (b) utilizing phenol as a single substrate to *in situ* generate cyclohexylphenol or cyclohexanone, in which the former reacts with phenol *via* alkylation and the latter undergoes self-condensation.

For route (a), with the presence of extra-added electrophilic reagents, the alkylation of phenol and electrophilic reagents can be easily achieved over an acid catalysts, leading to a high yield of multi-cyclic oxygenate precursors. Nie *et al.*[85] developed a one-pot synthesis of bi- and tricyclic cyclohexane from phenol with cyclopentanol through an enhanced alkylation followed by HDO over Pd/C+ Hβ dual catalysts, affording a high molar yield of 83.9% from the starting reactant (Table 7, entry 1). The mixture had a density of 0.89 g mL^{-1} at 20° C, net heat of combustion of 37.9 MJ L^{-1}, freezing point lower than −75 °C, and viscosity of 22.2 mm^2 s^{-1} at −40 °C. Its high-density characteristic makes it promising as an aviation jet fuel or additive.

Similarly, Shen *et al.*[94] developed a bifunctional Pt/Hβ catalyst for the one-pot conversion of phenol with cyclopentanol, which obtained an 83.4% yield of bicyclic and tricyclic cyclohexane in the final product (Table 7, entry 2). They found that the larger pore size of the alkali-treated Hβ would not limit the production of polycyclic compounds, and a good acid content in a particular mesoporous specific surface area could speed up the reaction rate. The bifunctional catalyst synthesized in this study makes it possible to synthesize fuels directly from lignin oil or other biomass molecules in a one-pot process.

For route (b), since dehydration reactions also occur at the acid active site, HDO and alkylation (or aldol condensation) are two competing pathways over metal–acid catalysts, even if the rate of alkylation (or aldol condensation) is much lower than the hydrogenation of aromatic rings. Scaldaferri *et al.*[102] observed that diphenyl ether hydrogenation occurs significantly more than C–C coupling reactions over Pd/OTS-HY catalysts. This is because C–C coupling must occur after hydrogenation and C–O cleavage of the reactants. If the metal function is too active compared to the acid function, it will increase the rate of secondary hydrogenation of the reactants, and the yield of the C–C coupling product will decrease. Therefore, it is important to balance the competition rate between the hydrogenation over the metal sites and the alkylation or aldol condensation over the acid sites.

García-Minguillán *et al.*[92] performed a one-pot synthesis of cyclohexylphenol *via* isopropanol-assisted phenol conversion

Table 7 Overview of the one-pot conversion of lignin C–O derivatives to polycycloalkanes[a]

Entry	Substrate	Conv. (%)	Catalyst	T (°C)	P (MPa)	t (h)	Solvent	Products	Sel./yield (%)	Ref.
1	Phenol	66.7	Pd/C	200	0.2 (N_2)	7	—	Bicyclic alkanes	74.3 (S)	85
	Cyclopentanol	100.0	HBEA		6.0 (H_2)			Tricyclic alkanes	16.2 (S)	
2	Phenol	83.0	Pt/Hβ	180	0.5 (N_2)	8	Decalin	Bicyclic & tricyclic	83.4 (Y)	94
	Cyclohexanol	100.0			0.5 (H_2)	8				
3	Guaiacol	100.0	Pd2%/Hβ	220	3 (H_2)	4	*n*-Hexane	Cycloalkane	39.8 (Y)	20
								Bicyclohexane	21.8 (Y)	
								(Cyclopentylmethyl)cyclohexane	16.0 (Y)	
4	Diphenyl ether	100.0	Ni10%/YBCZ	160	5 (H_2)	18	*n*-Pentane	Cycloalkane	87.9 (Y)	22
								Bicyclohexane	10.8 (Y)	
5	Cyclohexylphenol	100.0	Pd/C	150	4 (H_2)	30	H_2O	Bicyclohexane	62.0 (S)	87
			HZSM-5					(Cyclopentylmethyl)cyclohexane	32.0 (S)	
6	Diphenyl ether	97.0	Pd/HY	200	3.4 (H_2)	1	Decalin	Cycloalkane	36.0 (Y)	102
								[1′-Bicyclohexyl]-2-one	23.4 (Y)	
7	Guaiacol	98.7	Ni/Y	300	4 (H_2)	200 min	—	Cycloalkane	36.6 (S)	93
								Bicyclohexane	20.5 (S)	
8	Phenol	100.0	Pd/C	160	5 (H_2)	12	H_2O	Cycloalkane	40.0 (S)	96
			HBEA					Bicyclohexane	55.0 (S)	
9	Phenol	90.0	Co_2P/Beta	240	4 (H_2)	2	Decalin	Cycloalkane	54.0 (S)	103
								Cyclohexylphenol	34.0 (S)	
10	Phenol	60.0	Pd/C	200	4 (H_2)	4	H_2O	Hydroalkylation products	25.0 (Y)	104
			La-BEA							

[a] The molar yield and selectivity of polycycloalkane was calculated based on the C6 ring molar of initial substrate and product.

on a tandem catalytic system formed by RANEY®Ni plus hierarchical Beta zeolites. Under this tandem catalytic system, the synthesis of cyclohexylphenol was achieved with remarkable selectivity (~70%) and high conversion (64%) after 1 h of reaction at 150 °C. The hierarchical β-zeolite with more Brønsted acid sites and stronger Brønsted acid sites promoted the formation of cyclohexylphenol at a relatively low temperature compared to Al-SBA-15. However, the steric hindrance of micropore formation in ZSM-5 made it much less selective for cyclohexylphenol than H-Beta.

Gutiérrez-Rubio *et al.*[103] reported a one-pot hydroalkylation process to prepare cyclohexylphenol by loading Co_2P onto acidic zeolites using an impregnation method with phenol as the only organic substrate. The results showed that the highest phenol conversions were obtained over Co_2P/MCM-22 and Co_2P/Beta catalysts, which had the smallest Co_2P nanoparticles and the most considerable acid site accessibility due to their large mesoporous/external surface areas. The HDO/hydrogenation activity was weakened due to the formation of CoAlPO groups on the Co_2P/Beta catalysts. As a result, the extension of the phenol HDO/hydrogenation to cyclohexane/methylcyclopentane pathway was reduced, allowing the alkylation reaction between unconverted phenol and cyclohexene molecules to drive the system to form more cyclohexylphenol.

Hu *et al.*[20] prepared Pd-based zeolite catalysts for the HDO conversion of guaiacol using a modified deposition–precipitation (DP) method. The highest hydrocarbon production of guaiacol was achieved with Pd2%/Hβ (DP) catalysts, with a 39.79% cyclohexane yield and 21.84% bicyclohexane yield. For the same Si/Al ratio of zeolites, the catalytic activity of the Pd2%/Hβ catalyst for guaiacol HDO was higher than that of the Pd2%/M and Pd2%/HZSM-5 catalysts, which mainly originated from the synergistic effect between the metal nanoparticles and catalyst acid sites. Due to the presence of strong Lewis acid sites, the coupling reaction could significantly promote the rearrangement of cyclohexanone and cyclohexane to form bicyclohexyl-2-one. In addition, the coupling reaction also promoted the rearrangement of cyclohexane to polycycloalkanes, such as bicyclohexane.

Table 7 summarizes the state-of-the-art one-pot conversion of lignin C–O derivatives to polycycloalkanes. When adding cyclohexylphenol or cyclopentanol as electrophilic reagents to react with phenol, the C–C coupling was much easier to be carried out, leading to a high polycycloalkanes yield (>80%). When adopting phenol as a single substrate, the catalytic efficiency was relatively low due to the competition between the hydrogenation and C–C coupling, which generated monocycloalkanes as major products while the yield of polycycloalkanes was unsatisfactory (<50%). More studies should be performed on the catalyst design and on mechanism investigations to improve the production of polycycloalkanes.

3.4 Summary

In terms of the composition and jet-fuel performance, lignin-derived polycycloalkanes can generally meet the standards of jet fuel. Lignin-derived polycycloalkanes are mainly C9–C16 bicyclicalkanes, tricyclicalkanes, and condensed cycloalkanes.

These polycycloalkanes usually present a high fuel density up to 0.85 g mL^{-1}. However, other properties, such as the flash point, boiling point, freezing point, and viscosity, cannot be neglected. For example, when the carbon ring number exceeds 3, the density of the fuel exceeds 0.90 g mL^{-1}, but the freezing point and viscosity will both significantly increase, which is not conducive to use at low temperatures for aviation aircraft. Moreover, when the carbon number exceeds 20, the boiling point of cycloalkanes may exceed 300 °C. In fact, the final boiling point of the fuel needs to be limited to a maximum temperature of 300 °C to exclude the heavy compound fraction.[105] Therefore, the range of carbon rings and carbon numbers of jet fuel needs to be tightly controlled during fuel preparation in order to obtain the desired fuel performance. Some strategies can be adopted to improve the combination jet-fuel property of the lignin-derived polycycloalkanes. It has been reported that the introduction of alkyl substituents (especially methyl groups) to the carbon ring can decrease the freezing point of the fuel with a slightly decrease in fuel density too. Of course, through the combination of different lignin-derived polycycloalkanes, the fuel density and freezing point can be adjusted appropriately to realize the gradual improvement of the comprehensive performance of the fuel.

For polycycloalkanes production from lignin derivatives, the two-step routes, including the alkylation relay HDO route and the aldol condensation relay HDO route, present relatively high yields of polycycloalkanes, but two different catalytic systems are needed. As for the one-pot conversion route, the catalytic efficiency is relatively low at present due to the competition between the HDO and C–C coupling reaction in the same catalytic system, which generate monocycloalkanes as the major products while the yield of polycycloalkanes is unsatisfactory. Strategies such as adding cyclohexylphenol or cyclopentanol as electrophilic reagents into the catalytic system could facilitate the C–C coupling to realize a higher polycycloalkanes yield.

For the catalytic structure–activity relationship of the polycycloalkanes production system, current research has mostly focused on the design of reaction routes rather than the regulation of catalyst structures. Yet it was found that by adjusting the properties of the metal–acid catalyst, the competition between the HDO and C–C coupling reaction could be balanced to afford polycycloalkanes as the final products. More studies with a focus on the catalyst design and reaction mechanism could further promote the efficient production of polycycloalkanes from lignin derivatives.

4 Comparison of the direct HDO route to produce cycloalkanes and the C–C coupling relay HDO route to produce polycycloalkanes

4.1 Reaction pathways

As mentioned above, the production of cycloalkanes from the direct HDO of lignin derivatives requires the complete removal of oxygen and saturation of the benzene ring, and usually one-pot reactions are performed using efficient metal–acid catalysts, which can achieve a high yield of the target product. However, for the production of polycycloalkanes *via* the C–C coupling relay HDO route, the reaction pathway is more complicated and difficult to regulate. C–C coupling *via* alkylation or aldol condensation requires the simultaneous presence of electrophilic and nucleophilic intermediates, but these can usually be easily further converted into monocycloalkanes, resulting in a low yield of polycycloalkanes. Especially for the one-pot conversion of lignin derivatives without adding a coupling reagent, achieving the optimal the balance between hydrogenation and C–C coupling is still a major challenge.

4.2 Catalytic systems

The significant differences between reaction pathways make their respective suitable catalytic systems completely different. In the direct HDO system of lignin derivatives to cycloalkanes, catalysts with efficient hydrogen dissociation and C–O cleavage capacities are desired, and mainly include metal, metal–acid, sulfides, and phosphides catalysts. However, in the C–C coupling relay HDO system of lignin derivatives to polycycloalkanes, the catalysts for the C–C coupling step are strictly limited. It is generally agreed that the acid is the active site acting in the C–C coupling step. In addition to coupling, the acid site is also responsible for the cleavage of the C–O bond. Therefore, in the C–C coupling route, it is very important to regulate the acid sites. The choice of metal will also affect the acidic function to a certain extent, because a reasonable regulation of the ratio of metal to acid can increase the occurrence of alkylation reactions. Currently, in the catalytic system of the C–C coupling relay HDO, noble metals and zeolites play a more prominent role. This may be related to the good hydrogenation activity of noble metals and the adjustable acidity and pore sizes of the zeolites.

The pore size of the catalyst is also an important factor affecting the product. Smaller pore sizes with greater spatial obstruction allow only small molecular weight substances to pass through and are more suitable for the synthesis of monocycloalkanes. The synthesis of polycycloalkanes, on the other hand, requires larger pore sizes. The C–C coupling reactions are mostly carried out under milder conditions compared to the reaction conditions of HDO reactions. It is hypothesized that at high temperatures, the acidic sites would favor deoxygenation over C–C coupling.

5 Summary and perspectives

Lignin is a natural amorphous three-dimensional polymer with abundant C–O bonds and aromatic structures. These aromatic structures can act as bases to produce jet-fuel-range cycloalkanes *via* direct HDO and C–C coupling relay HDO, which are regarded as both short- and long-term solutions to replace fossil-crude-oil-derived jet fuel for the airline industry. This review systematically reviewed the latest achievements in

the catalytic preparation of cycloalkanes from lignin derivatives and real lignin. Although significant progress has been made in the research on the active sites, catalytic systems, structure–activity relationships, and catalytic mechanisms, there are still some challenges that require attention to improve the reaction efficiency as well as the product selectivity. These challenges include:

(i) More attention on the combination property of lignin-derived cycloalkanes. Cycloalkanes with different total carbon numbers, C6 ring numbers, and side chain substitutions present significant difference in fuel density, flash point, boiling point, freezing point, *etc*. In particular, jet-fuel-range cycloalkanes should meet strict standards on fuel density, freezing point, flash point, boiling point, *etc*. Therefore, more studies should be performed on the relationship between the fuel properties and fuel components, which could aid designing proper fuel molecules with a suitable fuel density, freezing point, and other properties.

(ii) Further development of bifunctional catalysts with non-noble metals. In the preparation system of cycloalkanes, noble metals have good hydrogenation activity and can obtain satisfactory results under mild reaction conditions. Moreover, noble metals are widely used to prepare polycycloalkanes, while the reaction conditions and catalytic steps limit the application of non-metal metals. Therefore, developing more efficient and milder non-noble metal catalysts deserves great attention. The catalytic activity and selectivity can be improved by adjusting the metal particle size, dispersion, and metal–support interactions. In addition, oxygenophilic metals have an affinity for oxygen-containing groups in phenolic compounds, which can help the cleavage of C–O bonds by adding oxygenophilic metals.

(iii) Reasonable regulation of the acid active sites. In the catalytic system of polycycloalkanes, the acid site can catalyze the C–C coupling reaction. However, at the same time, acid sites can also participate in dehydration. Once the dehydration reaction dominates, the possibility of the C–C coupling reaction decreases. In addition, the strength and number of acid sites should be appropriate. Too strong or too many acid sites is detrimental to the formation of the target product. Therefore, further studies are needed to regulate the acid sites to improve the target products' selectivity.

(iv) Focus on the synergistic effect between the metal and acid. The synergistic effect between the metal and acid is the focus of much research on bifunctional catalysts. The catalytic performance is usually better when the distance between the metal and acid sites is on the nanometer scale. This can be initiated with the preparation method of the catalyst, such as zeolite encapsulation. In addition, by adjusting the ratio of metal to acid sites, the yield of the target product can also be improved.

(v) Design of one-pot catalytic reactions. Most of the preparation pathways for monocycloalkanes are one-pot reactions. However, in the study of polycycloalkanes, cascade reactions are widely used because this reduces the catalytic difficulty. However, this process involves complex separation and purification of the target product at a high cost. From the principle of green economy, bifunctional catalysts are more attractive to catalyze the reaction sequentially in the same reactor.

(vi) In-depth investigation of the C–C coupling reaction mechanism. At present, alkylation and aldol condensation reactions are widely used in the study of the lignin preparation of polycycloalkanes. Reactions utilizing other C–C coupling mechanisms for catalytic synthesis are fewer. Therefore, catalytic pathways for the preparation of polycycloalkanes utilizing different C–C coupling mechanisms could be developed. In addition, the influence of the acidic site species in lignin C–C coupling needs to be clarified and requires further study.

Data availability

Data generated during the current study are available from the corresponding author upon reasonable request.

Conflicts of interest

There are no conflicts to declare.

Acknowledgements

This work was supported by National Natural Science Foundation of China (22178258, 22308254), China Postdoctoral Science Foundation (2023M742593, 2024T170642), Open Fund of the Key Laboratory of Functional Molecular Solids (FMS2023006), and the Independent Innovation Fund of Tianjin University (2024XQM-0021).

References

1 D. M. Alonso, J. Q. Bond and J. A. Dumesic, *Green Chem.*, 2010, **12**, 1493–1513.
2 X. Zhang, L. Zhang, J. Li, X. Zou, X. Jing and W. Li, *Fuel*, 2022, **325**, 124876.
3 W. J. Pitz and C. J. Mueller, *Prog. Energy Combust. Sci.*, 2011, **37**, 330–350.
4 W.-C. Wang and L. Tao, *Renewable Sustainable Energy Rev.*, 2016, **53**, 801–822.
5 M. J. Al Rashidi, M. Mehl, W. J. Pitz, S. Mohamed and S. M. Sarathy, *Combust. Flame*, 2017, **183**, 358–371.
6 H. Wei, W. Liu, X. Chen, Q. Yang, J. Li and H. Chen, *Fuel*, 2019, **254**, 115599.
7 A. Kumar, D. C. Bell, Z. Yang, J. Heyne, D. M. Santosa, H. Wang, P. Zuo, C. Wang, A. Mittal, D. P. Klein, M. J. Manto, X. Chen and B. Yang, *Fuel Process. Technol.*, 2024, **263**, 108129.
8 H. Ruan, Y. Qin, J. Heyne, R. Gieleciak, M. Feng and B. Yang, *Fuel*, 2019, **256**, 115947.
9 A. Li, Z. Zhang, X. Cheng, X. Lu, L. Zhu and Z. Huang, *Fuel*, 2020, **267**, 116975.

10 C. Song, S. Eser, H. H. Schobert and P. G. Hatcher, *Energy Fuels*, 1993, **7**, 234–243.
11 B. L. Smith and T. J. Bruno, *Energy Fuels*, 2007, **21**, 2853–2862.
12 K. Pearson, T. Käfer, G. Kraaij and A. Wörner, *Int. J. Hydrogen Energy*, 2015, **40**, 1367–1378.
13 F. Cheng and C. E. Brewer, *Renewable Sustainable Energy Rev.*, 2017, **72**, 673–722.
14 M. Lang and H. Li, *Fuel*, 2023, **344**, 128084.
15 R. Shu, R. Li, B. Lin, C. Wang, Z. Cheng and Y. Chen, *Biomass Bioenergy*, 2020, **132**, 105432.
16 G. Li, R. Wang, J. Pang, A. Wang, N. Li and T. Zhang, *Chem. Rev.*, 2024, **124**, 2889–2954.
17 L. Zhang, Y. Wang, Y. Yang, B. Zhang, S. Wang, J. Lin, S. Wan and Y. Wang, *Catal. Today*, 2021, **365**, 199–205.
18 W. Jiang, J.-P. Cao, N.-Y. Yao, J.-X. Xie, L. Zhao, F.-J. Yi, C. Zhang, C. Zhu, X.-Y. Zhao, Y.-P. Zhao and J.-L. Zhang, *Ind. Eng. Chem. Res.*, 2022, **61**, 2937–2946.
19 J. Resasco, F. Yang, T. Mou, B. Wang, P. Christopher and D. E. Resasco, *ACS Catal.*, 2020, **10**, 595–603.
20 L. Hu, X.-Y. Wei, M.-L. Xu, Y.-H. Kang, X.-H. Guo, F.-B. Zhang, Z.-M. Zong and H.-C. Bai, *J. Environ. Chem. Eng.*, 2021, **9**, 106599.
21 V. V. Pushkarev, K. An, S. Alayoglu, S. K. Beaumont and G. A. Somorjai, *J. Catal.*, 2012, **292**, 64–72.
22 X.-Q. Zhang, Y.-H. Kang, J. Gao, L. Xiong, Y. Gao, T. Chen, G.-H. Liu, A.-M. Wang, X.-Y. Wei, Z.-M. Zong and H.-C. Bai, *Fuel*, 2022, **321**, 124062.
23 S. Chen, C. Miao, Y. Luo, G. Zhou, K. Xiong, Z. Jiao and X. Zhang, *Renewable Energy*, 2018, **115**, 1109–1117.
24 Y.-H. Kang, X.-Y. Wei, J. Li, H. Jin, T. Li, C.-Y. Lu, X.-R. Ma and Z.-M. Zong, *Fuel*, 2021, **287**, 119396.
25 Y.-H. Kang, X.-Y. Wei, X.-Q. Zhang, Y.-J. Li, G.-H. Liu, X.-R. Ma, X. Li, H.-C. Bai, Z.-N. Li, H.-J. Yan and Z.-M. Zong, *Renewable Energy*, 2021, **173**, 876–885.
26 J. Zhang, J. Sun and Y. Wang, *Green Chem.*, 2020, **22**, 1072–1098.
27 C. Zhang, X. Zhang, J. Wu, L. Zhu and S. Wang, *Appl. Energy*, 2022, **328**, 120199.
28 Z. Wu, L. Hu, Y. Jiang, X. Wang, J. Xu, Q. Wang and S. Jiang, *Biomass Convers. Biorefin.*, 2023, **13**, 519–539.
29 A. M. Robinson, J. E. Hensley and J. W. Medlin, *ACS Catal.*, 2016, **6**, 5026–5043.
30 J. ten Dam and U. Hanefeld, *ChemSusChem*, 2011, **4**, 1017–1034.
31 P. Yan, J. Mensah, M. Drewery, E. Kennedy, T. Maschmeyer and M. Stockenhuber, *Appl. Catal., B*, 2021, **281**, 119470.
32 W. Jiang, J.-P. Cao, J.-X. Xie, L. Zhao, C. Zhang, X.-Y. Zhao, Y.-P. Zhao and J.-L. Zhang, *Energy Fuels*, 2021, **35**, 19543–19552.
33 M. Zabeti, W. M. A. Wan Daud and M. K. Aroua, *Fuel Process. Technol.*, 2009, **90**, 770–777.
34 M. Trueba and S. P. Trasatti, *Eur. J. Inorg. Chem.*, 2005, **2005**, 3393–3403.
35 C. Zhu, S. Ding, H. Hojo and H. Einaga, *ACS Catal.*, 2021, **11**, 12661–12672.
36 M. Zhou, J. Ye, P. Liu, J. Xu and J. Jiang, *ACS Sustainable Chem. Eng.*, 2017, **5**, 8824–8835.
37 M. O. Bengoechea, A. Hertzberg, N. Miletić, P. L. Arias and T. Barth, *J. Anal. Appl. Pyrolysis*, 2015, **113**, 713–722.
38 X. Zhang, W. Tang, Q. Zhang, T. Wang and L. Ma, *Appl. Energy*, 2018, **227**, 73–79.
39 L. Nie and D. E. Resasco, *J. Catal.*, 2014, **317**, 22–29.
40 V. B. F. Custodis, S. A. Karakoulia, K. S. Triantafyllidis and J. A. van Bokhoven, *ChemSusChem*, 2016, **9**, 1134–1145.
41 X. Zhang, T. Wang, L. Ma, Q. Zhang, X. Huang and Y. Yu, *Appl. Energy*, 2013, **112**, 533–538.
42 L. Dong, L. Lin, X. Han, X. Si, X. Liu, Y. Guo, F. Lu, S. Rudić, S. F. Parker, S. Yang and Y. Wang, *Chem*, 2019, **5**, 1521–1536.
43 J. Ballesteros-Soberanas, L. D. Ellis and J. W. Medlin, *ACS Catal.*, 2019, **9**, 7808–7816.
44 L. O. Mark, C. Zhu, J. W. Medlin and H. Heinz, *ACS Catal.*, 2020, **10**, 5462–5474.
45 S. Chen, W. Wang, X. Li, P. Yan, W. Han, T. Sheng, T. Deng, W. Zhu and H. Wang, *J. Energy Chem.*, 2022, **66**, 576–586.
46 W. Guan, C.-W. Tsang, C. S. K. Lin, C. Len, H. Hu and C. Liang, *Bioresour. Technol.*, 2020, **298**, 122432.
47 X. Huang, O. M. M. Gonzalez, J. Zhu, T. I. Korányi, M. D. Boot and E. J. M. Hensen, *Green Chem.*, 2017, **19**, 175–187.
48 N. Ji, S. Cheng, Z. Jia, H. Li, P. Ri, S. Wang and X. Diao, *ChemCatChem*, 2022, **14**, e202200274.
49 P. B. Weisz, in *Advances in Catalysis*, ed. D. D. Eley, P. W. Selwood, P. B. Weisz, A. A. Balandin, J. H. De Boer, P. J. Debye, P. H. Emmett, J. Horiuti, W. Jost, G. Natta, E. K. Rideal and H. S. Taylor, Academic Press, 1962, vol. 13, pp. 137–190.
50 Z. Yang, B. Luo, R. Shu, Z. Zhong, Z. Tian, C. Wang and Y. Chen, *Fuel*, 2022, **319**, 123617.
51 J. Zecevic, G. Vanbutsele, K. P. de Jong and J. A. Martens, *Nature*, 2015, **528**, 245–248.
52 W. Jiang, J.-P. Cao, Z. Yang, J.-X. Xie, L. Zhao, C. Zhu, C. Zhang, X.-Y. Zhao, Y.-P. Zhao and J.-L. Zhang, *Ind. Eng. Chem. Res.*, 2022, **61**, 2937–2946.
53 Q. Chen, C. Cai, X. Zhang, Q. Zhang, L. Chen, Y. Li, C. Wang and L. Ma, *ACS Sustainable Chem. Eng.*, 2020, **8**, 9335–9345.
54 H. Wang, H. Ruan, M. Feng, Y. Qin, H. Job, L. Luo, C. Wang, M. H. Engelhard, E. Kuhn, X. Chen, M. P. Tucker and B. Yang, *ChemSusChem*, 2017, **10**, 1846–1856.
55 Z. Zhong, J. Li, M. Jian, R. Shu, Z. Tian, C. Wang, Y. Chen, N. Shi and Y. Wu, *Fuel*, 2023, **333**, 126241.
56 C. Ju, M. Li, Y. Fang and T. Tan, *Green Chem.*, 2018, **20**, 4492–4499.
57 J. Yang, Y. He, J. He, Y. Liu, H. Geng, S. Chen, L. Lin, M. Liu, T. Chen, Q. Jiang, B. M. Weckhuysen, W. Luo and Z. Wu, *ACS Catal.*, 2022, **12**, 1847–1856.
58 P. He, Q. Yi, H. Geng, Y. Shao, M. Liu, Z. Wu, W. Luo, Y. Liu and V. Valtchev, *ACS Catal.*, 2022, **12**, 14717–14726.

59 D. Farrusseng and A. Tuel, *New J. Chem.*, 2016, **40**, 3933–3949.
60 L. Shuai, J. Sitison, S. Sadula, J. Ding, M. C. Thies and B. Saha, *ACS Catal.*, 2018, **8**, 6507–6512.
61 X. Kong, C. Liu, H. Zeng, Y. Fan, H. Zhang and R. Xiao, *ChemSusChem*, 2024, **17**, e202300996.
62 Z. Luo, C. Liu, A. Radu, D. F. de Waard, Y. Wang, J. T. Behaghel de Bueren, P. D. Kouris, M. D. Boot, J. Xiao, H. Zhang, R. Xiao, J. S. Luterbacher and E. J. M. Hensen, *Natl. Chem. Eng.*, 2024, **1**, 61–72.
63 H. Wang, H. Ruan, H. Pei, H. Wang, X. Chen, M. P. Tucker, J. R. Cort and B. Yang, *Green Chem.*, 2015, **17**, 5131–5135.
64 Y. Shao, Q. Xia, L. Dong, X. Liu, X. Han, S. F. Parker, Y. Cheng, L. L. Daemen, A. J. Ramirez-Cuesta, S. Yang and Y. Wang, *Nat. Commun.*, 2017, **8**, 16104.
65 Q. Xia, Z. Chen, Y. Shao, X. Gong, H. Wang, X. Liu, S. F. Parker, X. Han, S. Yang and Y. Wang, *Nat. Commun.*, 2016, **7**, 1–10.
66 G. F. Leal, S. Lima, I. Graça, H. Carrer, D. H. Barrett, E. Teixeira-Neto, A. A. S. Curvelo, C. B. Rodella and R. Rinaldi, *iScience*, 2019, **15**, 467–488.
67 X. Li, B. Zhang, X. Pan, J. Ji, Y. Ren, H. Wang, N. Ji, Q. Liu and C. Li, *ChemSusChem*, 2020, **13**, 4409–4419.
68 Standard Specification for Aviation Turbine Fuel Containing Synthesized Hydrocarbons, ASTM D7566.
69 E. E. Peiffer, J. S. Heyne and M. B. Colket, in *2018 Joint Propulsion Conference*, American Institute of Aeronautics and Astronautics.
70 Z. Yang, Z. Xu, M. Feng, J. R. Cort, R. Gieleciak, J. Heyne and B. Yang, *Fuel*, 2022, **321**, 124040.
71 X. Wang and R. Rinaldi, *Angew. Chem., Int. Ed.*, 2013, **52**, 11499–11503.
72 X. Diao, N. Ji, X. Li, Y. Rong, Y. Zhao, X. Lu, C. Song, C. Liu, G. Chen, L. Ma, S. Wang, Q. Liu and C. Li, *Appl. Catal., B*, 2022, **305**, 121067.
73 Z. Luo, J. Kong, B. Ma, Z. Wang, J. Huang and C. Zhao, *ACS Sustainable Chem. Eng.*, 2020, **8**, 2158–2166.
74 Z. Luo, S. Qin, S. Chen, Y. Hui and C. Zhao, *Green Chem.*, 2020, **22**, 1842–1850.
75 S. Qin, B. Li, Z. Luo and C. Zhao, *Green Chem.*, 2020, **22**, 2901–2908.
76 S. Kasakov, H. Shi, D. M. Camaioni, C. Zhao, E. Baráth, A. Jentys and J. A. Lercher, *Green Chem.*, 2015, **17**, 5079–5090.
77 Z. Jia, N. Ji, X. Diao, X. Li, Y. Zhao, X. Lu, Q. Liu, C. Liu, G. Chen, L. Ma, S. Wang, C. Song and C. Li, *ACS Catal.*, 2022, **12**, 1338–1356.
78 Z. Dou, Z. Zhang, H. Zhou and M. Wang, *Angew. Chem., Int. Ed.*, 2021, **60**, 16399–16403.
79 H. Duan, J. Dong, X. Gu, Y.-K. Peng, W. Chen, T. Issariyakul, W. K. Myers, M.-J. Li, N. Yi, A. F. R. Kilpatrick, Y. Wang, X. Zheng, S. Ji, Q. Wang, J. Feng, D. Chen, Y. Li, J.-C. Buffet, H. Liu, S. C. E. Tsang and D. O'Hare, *Nat. Commun.*, 2017, **8**, 591.
80 L. Dong, Y. Shao, X. Han, X. Liu, Q. Xia, S. F. Parker, Y. Cheng, L. L. Daemen, A. J. Ramirez-Cuesta, Y. Wang and S. Yang, *Catal. Sci. Technol.*, 2018, **8**, 6129–6136.
81 X. Jiang, G. He, X. Wu, Y. Guo, W. Fang and L. Xu, *J. Chem. Eng. Data*, 2014, **59**, 2499–2504.
82 J. Zhao, B. Zhao, X. Wang and X. Yang, *Int. J. Hydrogen Energy*, 2017, **42**, 18626–18632.
83 A. Olivas, E. Gaxiola, J. Cruz-Reyes, M. A. Alvarez-Amparán and R. Valdez, *Fuel Process. Technol.*, 2020, **204**, 106410.
84 M. M. Ambursa, L. H. Voon, J. J. Ching, Y. Yahaya and J. N. Appaturi, *Fuel*, 2019, **236**, 236–243.
85 G. Nie, Y. Dai, Y. Liu, J. Xie, S. Gong, N. Afzal, X. Zhang, L. Pan and J.-J. Zou, *Chem. Eng. Sci.*, 2019, **207**, 441–447.
86 C. Zhao and J. A. Lercher, *Angew. Chem., Int. Ed.*, 2012, **51**, 5935–5940.
87 G. Nie, Y. Dai, J. Xie, X. Zhang, L. Pan and J.-J. Zou, *Catal. Today*, 2021, **365**, 235–240.
88 W. F. Seyer and C. H. Davenport, *J. Am. Chem. Soc.*, 1941, **63**, 2425–2427.
89 A. J. Streiff, L. F. Soule, C. M. Kennedy, M. E. Janes, V. A. Sedlak, C. B. Willingham and F. D. Rossini, *J. Res. Natl. Bur. Stand.*, 1950, **45**, 173.
90 M. H. Gollis, L. I. Belenyessy, B. J. Gudzinowicz, S. D. Koch, J. O. Smith and R. J. Wineman, *J. Chem. Eng. Data*, 1962, **7**, 311–316.
91 G. Nie, H. Wang, Q. Li, L. Pan, Y. Liu, Z. Song, X. Zhang, J.-J. Zou and S. Yu, *Appl. Catal., B*, 2021, **292**, 120181.
92 A. M. García-Minguillán, L. Briones, M. Alonso-Doncel, J. Čejka, D. P. Serrano, J. A. Botas and J. M. Escola, *Green Chem.*, 2022, **24**, 9168–9179.
93 P. Yan, G. Bryant, M. M.-J. Li, J. Mensah, E. Kennedy and M. Stockenhuber, *Microporous Mesoporous Mater.*, 2020, **309**, 110561.
94 Z. Shen, G. Zhang, C. Shi, J. Qu, L. Pan, Z. Huang, X. Zhang and J.-J. Zou, *Fuel*, 2023, **334**, 126634.
95 G. Nie, X. Zhang, P. Han, J. Xie, L. Pan, L. Wang and J.-J. Zou, *Chem. Eng. Sci.*, 2017, **158**, 64–69.
96 C. Zhao, D. M. Camaioni and J. A. Lercher, *J. Catal.*, 2012, **288**, 92–103.
97 Z. Li, L. Pan, G. Nie, J. Xie, J. Xie, X. Zhang, L. Wang and J.-J. Zou, *Chem. Eng. Sci.*, 2018, **191**, 343–349.
98 J. Xu, N. Li, G. Li, F. Han, A. Wang, Y. Cong, X. Wang and T. Zhang, *Green Chem.*, 2018, **20**, 3753–3760.
99 X. Zhang, F. Han, S. Lin, F. Chen, M.-J. Sun, J. Liu, G. Li, H. Tang, A. Wang and N. Li, *ACS Sustainable Chem. Eng.*, 2019, **7**, 12023–12031.
100 H. Liu, T. Jiang, B. Han, S. Liang and Y. Zhou, *Science*, 2009, **326**, 1250–1252.
101 J. Sun, S. Shao, X. Hu, X. Li and H. Zhang, *ACS Sustainable Chem. Eng.*, 2022, **10**, 11030–11040.
102 C. A. Scaldaferri, P. Warakunwit, V. M. D. Pasa and D. E. Resasco, *Appl. Catal., B*, 2019, **259**, 118081.
103 S. Gutiérrez-Rubio, M. Shamzhy, J. Čejka, D. P. Serrano, J. M. Coronado and I. Moreno, *Catal. Today*, 2022, **390–391**, 135–145.
104 C. Zhao, W. Song and J. A. Lercher, *ACS Catal.*, 2012, **2**, 2714–2723.
105 J. Yang, Z. Xin, Q. (Sophia) He, K. Corscadden and H. Niu, *Fuel*, 2019, **237**, 916–936.

